Journal of Medicinal Chemistry

ARTICLE

pubs.acs.org/jmc

N-Cyclic Bay-Substituted Perylene G-Quadruplex Ligands Have Selective Antiproliferative Effects on Cancer Cells and Induce Telomere Damage

Valentina Casagrande,[†] Erica Salvati,[‡] Antonello Alvino,[†] Armandodoriano Bianco,[†] Alina Ciammaichella,[†] Carmen D'Angelo,[‡] Luca Ginnari-Satriani,[†] Anna Maria Serrilli,[†] Sara Iachettini,[‡] Carlo Leonetti,[‡] Stephen Neidle,[§] Giancarlo Ortaggi,[†] Manuela Porru,[‡] Angela Rizzo,[‡] Marco Franceschin,[†,*] and Annamaria Biroccio[‡,*]

[†]Dipartimento di Chimica, Università degli Studi "La Sapienza", P.le A. Moro 5, 00185 Roma, Italy

[‡]Experimental Chemotherapy Laboratory, Regina Elena Cancer Institute, Via delle Messi d'Oro 156, 00158 Rome, Italy

[§]Cancer Research UK Biomolecular Structure Group, The School of Pharmacy, University of London, London, U.K.

ABSTRACT: A series of bay-substituted perylene derivatives is reported as a new class of G-quadruplex ligands. The synthesized compounds have differing *N*-cyclic substituents on the bay area and differing side chains on the perylene major axis. ESI-MS and FRET measurements highlighted the strongest quadruplex binders in this series and those showing the highest quadruplex/duplex selectivity. Several biological assays were performed on these compounds, which showed that compound **5** (PPL3C) triggered a DNA damage response in transformed cells with the formation of telomeric foci containing phosphorylated γ-H2AX and 53BP1. This effect mainly occurred in replicating cells and was consistent with Pot1 dissociation. Compound **5** does not induce telomere damage in normal cells, which are unaffected by treatment with the compound, suggesting that this agent preferentially kills cancer cells. These results reinforce the notion that G-quadruplex binding compounds can act as broad inhibitors of telomere-related processes and have potential as selective antineoplastic drugs.

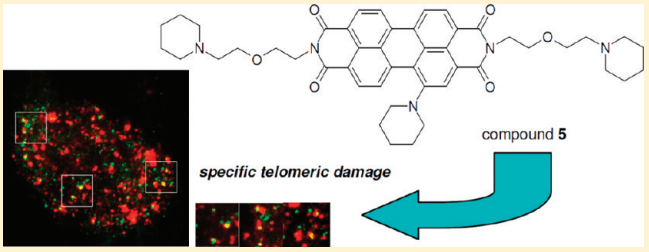

INTRODUCTION

In the expanding field of G-quadruplex nucleic acid structures,[1] particular attention has been devoted to their role in key biological processes,[2] especially for oncogene promoters and telomeres.[3] These findings have prompted the search for small organic molecules as specific ligands for these structures for development as potential anticancer agents.[4] These G-quadruplex ligands are usually characterized by an aromatic core that favors stacking interactions with the G-tetrads and, in most cases, by basic side chains (positively charged in physiological conditions), which interact with the quadruplex grooves and loops.[5] Some of these molecules have also been shown to induce telomere shortening and/or telomere instability, triggering apoptosis and/or senescence programs in various cell lines[6] and in some cases perturbing the equilibrium of capped/uncapped telomeres.[7] Two drugs that either target a G-quadruplex (Quarfloxin) or fold into a G-quadruplex structure (AS1411) are in phase II clinical trials.[8] Intriguingly, both drugs seem to exert their effect through nucleolin. G-quadruplex-interactive molecules acting on telomeres are still in preclinical development. Therefore, identification of new telomere-interactive molecules having antitumor effects is still a major challenge.

Perylene derivatives possess several optimal features to interact with G-quadruplexes, having a large hydrophobic moiety with the possibility of readily varying the number and nature of the hydrophilic side chains.[9] They have been shown to be able to induce different G-quadruplex structures and to inhibit human telomerase in vitro,[10] depending on the side chain basicity and length.[11] Other than simple perylene diimides with two basic side chains, we have previously reported a series of highly hydrosoluble perylene derivatives with three or four side chains.[12] Bay-substituted perylene derivatives are very soluble in aqueous media, and their tendency to self-aggregate is remarkably reduced compared to the previously reported two-chain perylene diimides.[12a] They exhibit enhanced ability to interact with G-quadruplex structures and to inhibit human telomerase compared to the previously reported perylene derivatives.[12b]

Different substitution on the bay area, using cyclic secondary amines, led to the preparation of different bay-substituted perylene diimides, such as **15** (PIP-PIPER(1,7)).[13] This compound is very selective for G-quadruplex structures rather than duplex DNA as shown by ESI mass spectrometry and is distinct from three- and four-chained perylene derivatives, which are poorly selective.[14d] On the other hand, the absolute affinity of **15** for G-quadruplex DNA is not very high, in particular for human telomeric sequences.[14d] We report here on a series of structurally

Received: July 20, 2010
Published: January 31, 2011

dx.doi.org/10.1021/jm1013665 | *J. Med. Chem.* 2011, 54, 1140–1156

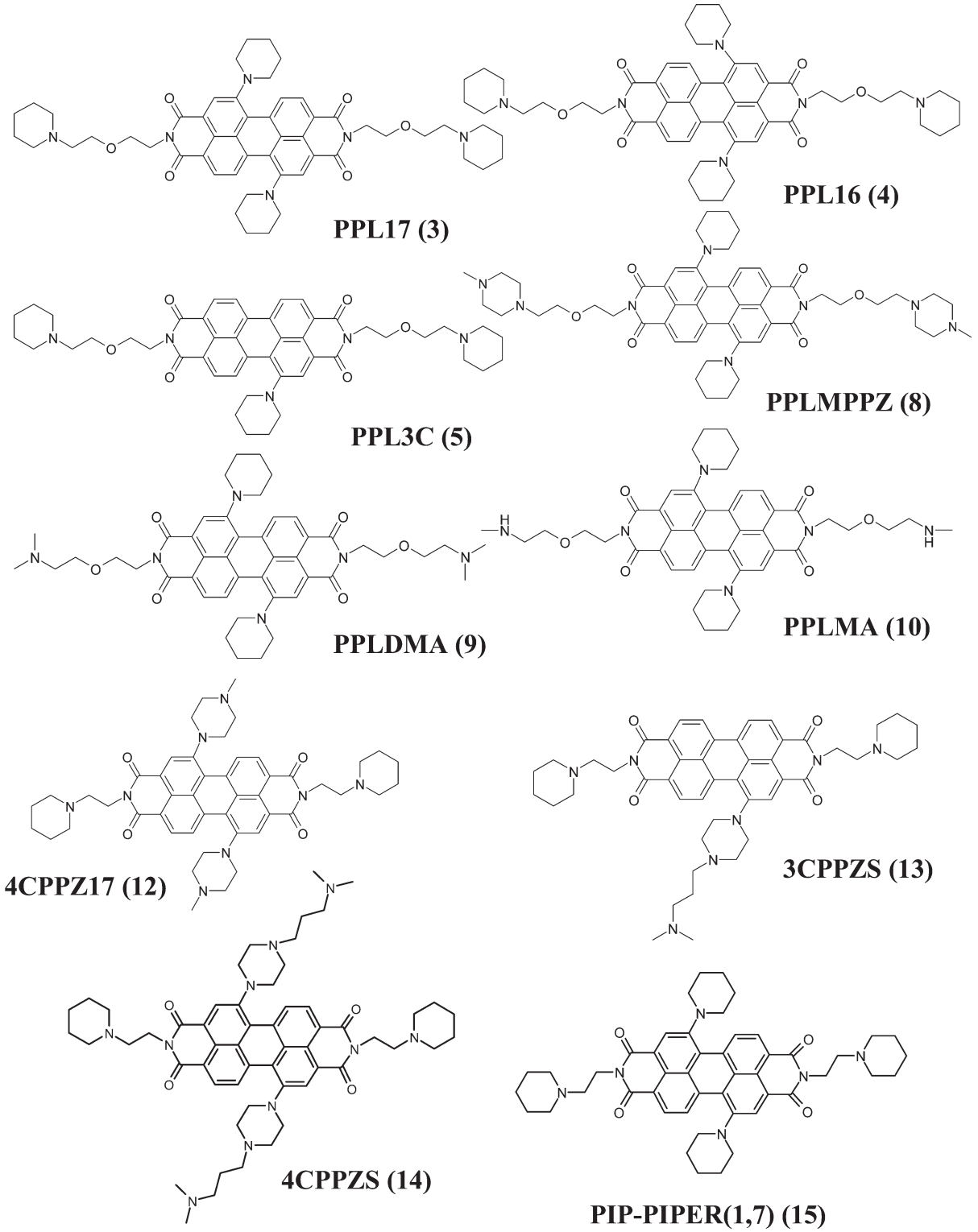

Figure 1. Structures of the synthesized molecules and reference compound PIP-PIPER(1,7).[13] All compounds used in the biophysical and biological evaluations were prepared as hydrochlorides as described in the Experimental Section.

related perylene derivatives (Figure 1), with different *N*-cyclic substituents in the bay area and different side chains on the perylene major axis, in order to obtain G-quadruplex ligands of enhanced affinity with respect to the reference compound **15** but with selectivity maintained. Specific biological assays have been performed on the best compounds of the series, as found by ESI-MS and FRET measurements, to determine their in vitro and in vivo effects, with particular attention to their specificity.

RESULTS AND DISCUSSION

Synthesis. Our design strategy starts from the general conclusion that perylene diimides with longer, flexible, and hydrophilic side

dx.doi.org/10.1021/jm1013665 |*J. Med. Chem.* 2011, 54, 1140–1156

Scheme 1. Synthesis of Compounds 3, 4, and 5

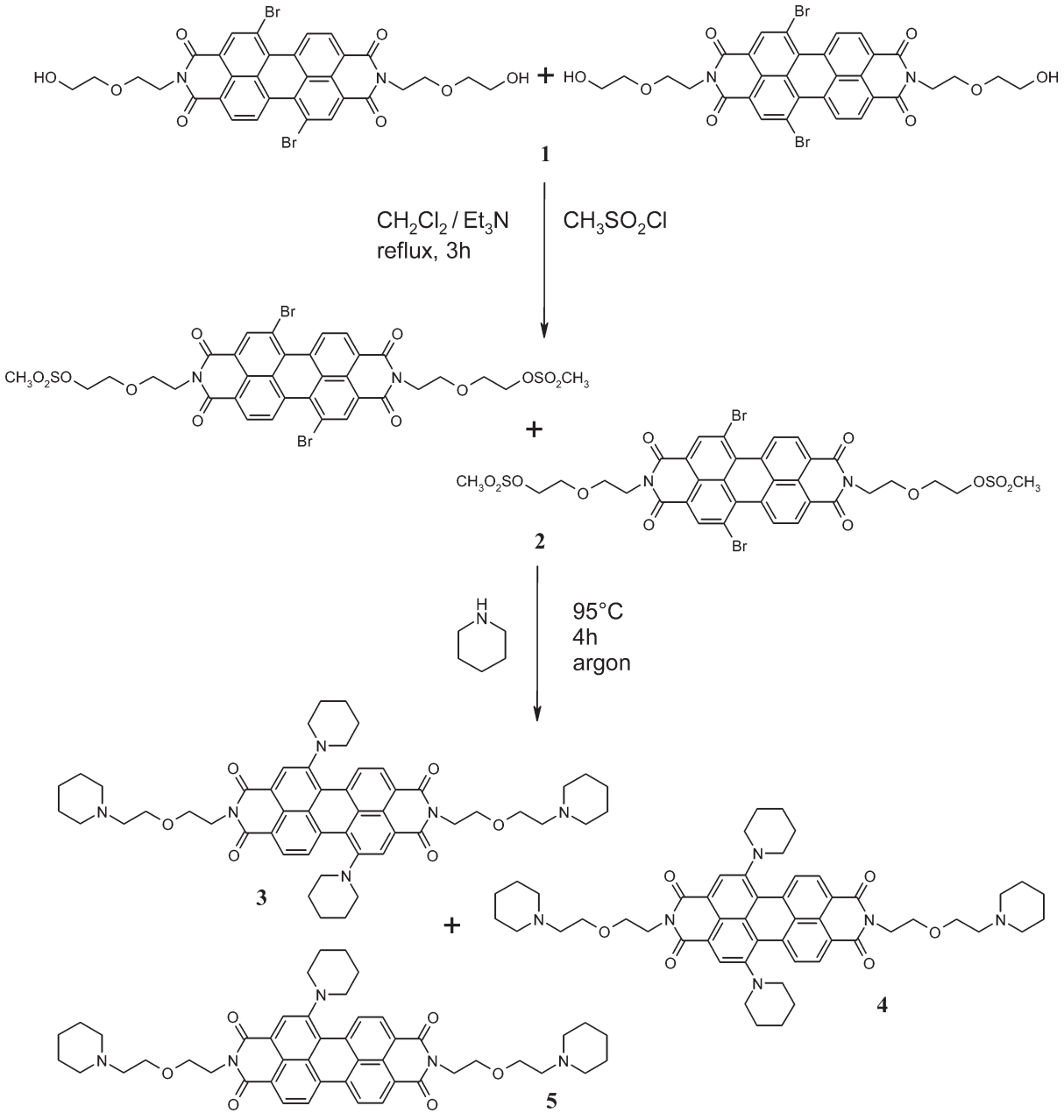

chains are more active both as G-quadruplex ligands and telomerase inhibitors[10,11] compared to derivatives having shorter hydrocarbon linkers in the side chains. The first modification we have made to the structure of **15** has been the insertion of oxygen-containing side chains on the major axis of perylene (compounds **3**−**5**). We used **1** (PEOE-Br) as a starting point which has been previously prepared by reaction of dibromo-perylene-tetracarboxylic dianhydride with commercially available 2-(2-aminoethoxy)ethanol (data to be published). We obtained a mixture of two isomers (1,6 and 1,7), and no side product involving the reaction of hydroxyl groups with the cyclic anhydride was detected.

Treatment of **1** with methanesulfonyl chloride in a 1:2 ratio gave quantitative conversion to the intermediate compound **2**, which is readily available for subsequent nucleophilic substitution. Both the methanesulfonyl groups and the bromine atoms on the perylene bay area were substituted by reaction with a large excess of piperidine (Scheme 1). This reaction gave three products that were successfully separated by column chromatography: the two isomers **3** (PPL17) and **4** (PPL16), together with **5** (PPL3C), a derivative obtained by partial dehalogenation of the dibromo diimide, a side reaction that has also been described in the literature.[15] The product of dehalogenation increased with temperature; this reaction may involve a free radical mechanism.

A different strategy was used in order to obtain perylene derivatives with different end groups on the perylene major axes (compounds **8**−**10**), with the aim of modulating interaction with quadruplex DNA grooves,[10,11] in particular having a N−H group able to form further hydrogen bonds and a piperazine containing

dx.doi.org/10.1021/jm1013665 |*J. Med. Chem.* 2011, 54, 1140–1156

Scheme 2. Synthesis of Compounds 8, 9, and 10

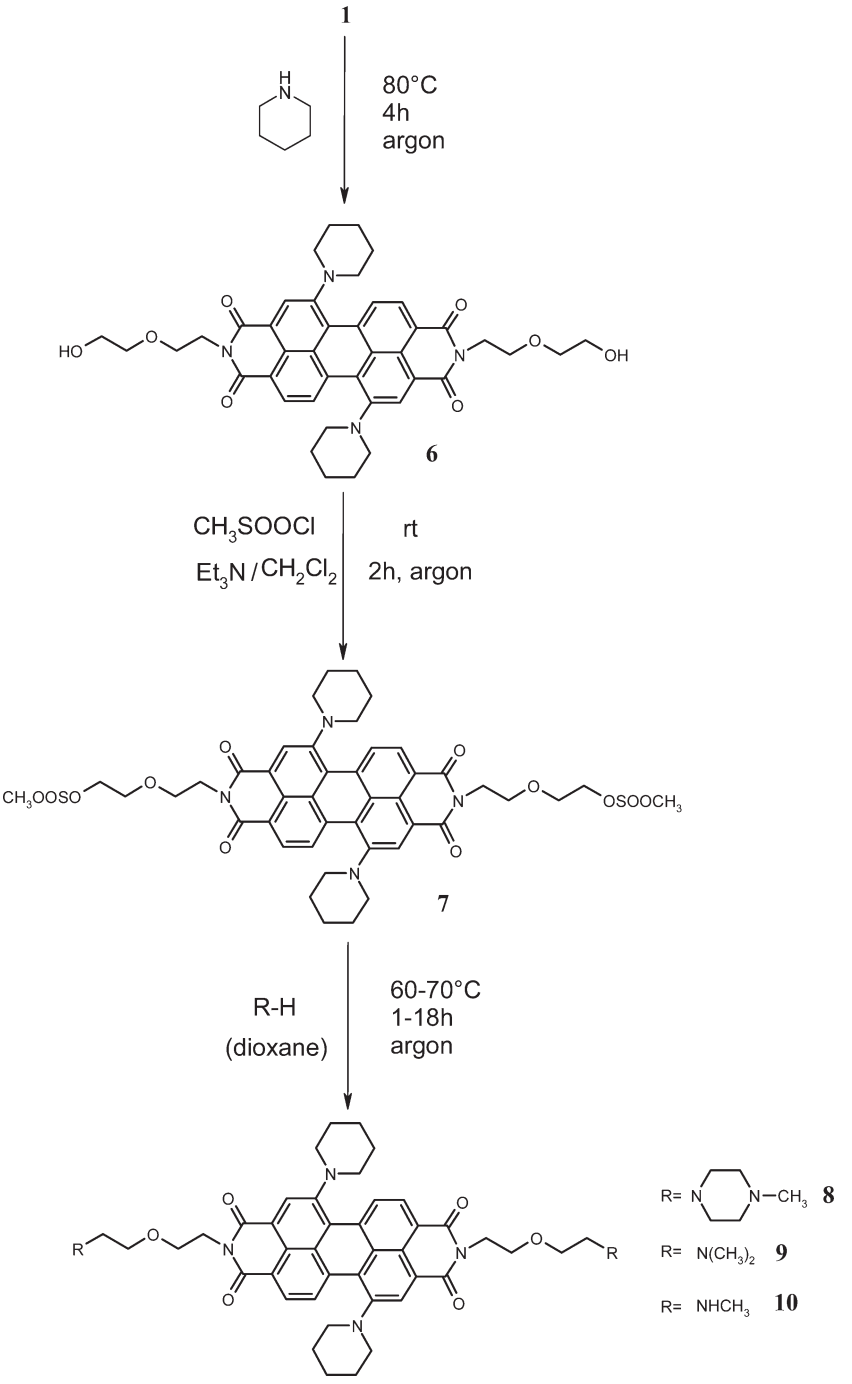

two aminic groups (Scheme 2). The same starting compound **1** was initially treated with a large excess of piperidine, displacing bromine atoms in the bay area and giving the intermediate compound **6**, while in these conditions the hydroxyl groups of the side chains are unaffected. As previously reported,[13] the insertion of N-substituents in the bay area facilitated the isolation of the main 1,7 isomer from the corresponding 1,6 isomer by column chromatography. Analogously to what has been reported above, treatment of the pure isomer **6** with methanesulfonyl chloride in a 1:2 ratio gave quantitative conversion to the intermediate compound **7**. The terminal groups of the side chains of this compound can be easily converted to the desired amino group by reaction with the appropriate primary or secondary amine, without affecting the perylene bay area, which retains the piperidine group, cf. compound **15**. Three different amines were used to perform substitution of the mesylate groups: 1-methylpiperazine, dimethylamine, and methylamine. The reaction conditions were different depending on the physical state of the reactant: 1-methylpiperazine was used as a solvent, while in the other cases the gaseous amine was added as a solution

dx.doi.org/10.1021/jm1013665 |*J. Med. Chem.* 2011, 54, 1140–1156

Scheme 3. Synthesis of Compounds 12, 13, and 14

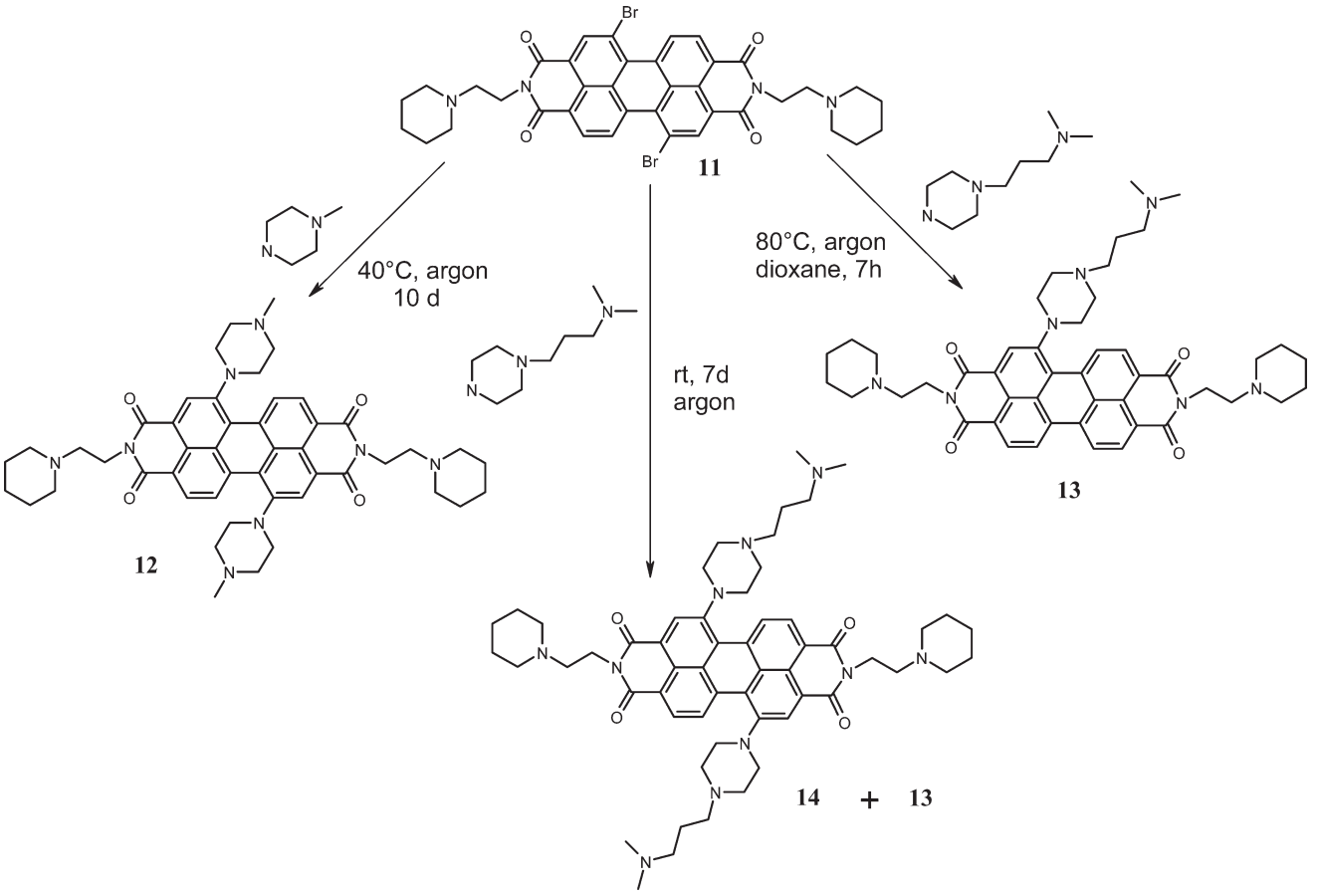

(in water or THF) and dioxane was used as a solvent. Reaction times and temperature were optimized as described in the Experimental Section to obtain three new perylene derivatives: **8** (PPLMPPZ), **9** (PPLDMA), and **10** (PPLMA) (Scheme 2).

The last group of perylene diimides synthesized has the same side chains as **15** on the perylene major axis but different *N*-cyclic substituents on the minor axis (compounds **12**−**14**). In particular, piperazine building blocks were used on the basis of the finding that more basic groups and a greater number of side chains on the perylene core generally improves the activity of this class of compounds.[10−12] These molecules have been synthesized starting from **11** (PIPER-Br), which we have previously described.[13] This compound has two bromine atoms in the bay area, while the two side chains as in PIPER[10] and **15** have been already inserted. So it was possible to replace the bromine atoms with different secondary amines (Scheme 3). The chosen amines were 1-methyl-piperazine and 1-(3-dimethylaminopropyl)piperazine; both are cyclic, which in our view is an important factor in order to optimize selectivity between quadruplex and duplex structures and are characterized by the presence of more than one amine group, which could increase electrostatic interactions between ligands and quadruplex DNA. In general, these reactions presented several additional synthetic problems compared to the other synthetic schemes. We noticed that the presence of an increasing number of amine groups had an influence on reaction yields, favoring the dehalogenation side reactions. To avoid this problem in the case of the reaction with a large excess of 1-methylpiperazine, it was necessary to reduce the temperature to 40 °C, extending the reaction time to 10 days; in this way compound **12** (4CPPZ17) was synthesized (Scheme 3, left). Performing the same reaction with an excess of 1-(3-dimethylaminopropyl)piperazine, established that side reactions also occurred at room temperature, distinct from what was observed in all other cases. In this instance, the addition of anhydrous dioxane as solvent enabled the reaction to take place at a higher temperature and in a few hours, giving only **13** (3CPPZS) (Scheme 3, right).

When using 1-(3-dimethylaminopropyl)piperazine as a solvent and protracting the reaction for 7 days at room temperature, other than a minor amount of **13**, compound **14** (4CPPZS) was isolated and characterized (Scheme 3, center) but the low yield did not allow us to convert it into its hydrochloride and to undertake chemical and biological assays in aqueous solution. However, we decided not to persist in testing other reaction conditions because we noticed that the fourth side chain does not significantly increase G-quadruplex affinity because only three chains are able to insert into the DNA grooves[12b] on account of the perylene core size.

All the other synthesized compounds were converted into the respective water-soluble hydrochlorides by precipitation with diethyl ether from an acidic (HCl) solution of methanol, as described in the Experimental section.

Ligand Binding to Quadruplex and Duplex DNA by Electrospray Ionization Mass Spectrometry (ESI-MS). ESI-MS can be used to study the binding to quadruplex and duplex DNA.[14] We have previously reported[14d] that **15** had very high selectivity for the G-quadruplex structure formed by $(TG_4T)_4$. This oligonucleotide

Table 1. Values[a] of the Association Constants K_1 and K_2 and Percentage of Bound DNA as Derived by ESI-MS Experiments for G-Quadruplex (21-TT Oligo) and Duplex DNA (DK66 Oligo)

	21-TT					DK66				
compd	Log K_1	Log K_2	bound DNA (5:5)[b]	bound DNA (5:10)[b]	bound DNA (5:20)[b]	Log K_1	Log K_2	bound DNA (5:5)[b]	bound DNA (5:10)[b]	bound DNA (5:20)[b]
3	4.7 ± 0.1	4.8 ± 0.1	23 ± 3	34 ± 2		4.2 ± 0.2				20 ± 5
4	4.8 ± 0.2	4.8 ± 0.1	20 ± 4	30 ± 2		3.8 ± 0.2				11 ± 4
5	5.8 ± 0.2	5.0 ± 0.1	56 ± 7	75 ± 6		3.9 ± 0.2	4.2 ± 0.1			21 ± 1
8	3.9 ± 0.2				15 ± 5	3.8 ± 0.1				10 ± 2
9	4.6 ± 0.2	4.9 ± 0.2	22.5 ± 0.4	30 ± 6		4.0 ± 0.2				16 ± 5
10	4.6 ± 0.2	4.8 ± 0.2	13 ± 4	37 ± 3		3.7 ± 0.2				9 ± 3
12	5.4 ± 0.2	5.6 ± 0.1	45 ± 3	77 ± 2		4.9 ± 0.3	4.2 ± 0.3	27 ± 2	44 ± 7	
13	5.5 ± 0.2	5.0 ± 0.2	48 ± 5	76 ± 7		5.4 ± 0.2	4.9 ± 0.2	43 ± 8	66 ± 6	
15	4.8 ± 0.1	4.6 ± 0.1	22 ± 3	33 ± 3		3.8 ± 0.1				12 ± 2

[a] Standard deviations are reported over at least three independent experiments. [b] Percentage (%) of bound DNA for experiments performed at the indicated DNA/drug ratios.

forms a simple tetramolecular G-quadruplex DNA, with no loops and having fully exposed terminal G-tetrads. This sequence was used for preliminary screening but is not biologically relevant to human telomeres. On the other hand, we found that **15** binds weakly to the 21-mer human telomeric sequence with also lower selectivity as there is only a small difference between duplex and quadruplex binding constants. This suggests that the presence of the cyclic substituents on the bay area of this molecule resulted in reduced capability to insert itself in the duplex grooves compared to binding to quadruplex DNA probably for steric reasons. The structural modifications of the new compounds, as discussed above, were aimed at increasing affinity for the intramolecular human telomeric quadruplex structure while maintaining the high degree of selectivity shown by **15** for $(TG_4T)_4$.

For these reasons, the new compounds have been tested with 21-TT and DK66 oligos, the former being a 21-mer human telomeric sequence and the latter a duplex-forming self-complementary dodecamer. The logarithms of the binding constants for the two association steps and the percentage of bound DNA are reported in Table 1. The latter parameter represents the percentage of DNA bound to ligand and enables one to readily compare ligands with differing behavior in terms of mode and stoichiometry of binding to DNA. As previously shown for other G-quadruplex ligands,[14d] the compounds studied are able to form both 1:1 and 2:1 drug−DNA complexes, in agreement with the general model of G-quadruplex-ligand interaction characterized by the presence of two binding sites on the external G-tetrad surfaces of the G-quadruplex structures.[5] The data show that almost all the tested molecules have comparable or significantly higher binding constants values for the G-quadruplex compared to **15**, with the exception of **8**. This compound showed weaker interaction and, at the concentrations used in these experiments, did not form 2:1 complexes.

In particular, it was found that by contrast with the simple perylene diimides having two side chains,[10,11] length modification of the major axis side chains (**3** and **4**) did not result in major changes in affinity to the human telomeric intramolecular quadruplex structure. Also, changing the end groups (**8**, **9**, and **10**) did not result in improved affinity for this quadruplex. By contrast, modifying the group directly bound to the bay area, by the insertion of cyclic substituents having more than one amine group, has a major influence on the activity of the perylene derivatives as G-quadruplex ligands. Both compounds with bay area piperazinyl substituents (**12** and **13**) have significantly higher affinity toward 21-TT compared to **15**, having greater than 2-fold more compound bound to the quadruplex DNA. However, the amount of duplex oligonucleotide bound for these two compounds was also high, in particular for **13**, suggesting poor quadruplex selectivity. Nevertheless, we have demonstrated that interactions with duplex oligonucleotides can occur so that before drawing conclusions about the biological selectivity of a compound it is necessary to obtain more information on its behavior in the presence of genomic DNA.[14d]

The most surprising results were those obtained for **5**. Despite its structural similarity with **3** and **4**, the lack of a piperidinyl group on the bay area has a noticeable effect on its quadruplex binding capability. Both binding constants for **5**, K_1 and K_2, are >10-fold greater compared to the two isomers **3** and **4**. This is probably due to reduced steric hindrance that enables improved overlap on the terminal G-tetrad to occur. On the other hand, **5** selectively binds quadruplex DNA and shows, as does **15**, poor affinity toward DK66, and a binding constant for the 1:1 complex 2 orders of magnitude lower compared to the quadruplex. These data enables us to deduce further structure−activity relationship data: only one piperidinyl group is necessary to enable the perylene core to become inserted in duplex grooves, while the second piperidinyl group only hinders interaction with the terminal quadruplex G-tetrad.

A more reliable analysis of quadruplex vs duplex selectivity has been undertaken on a selection of the new molecules in the simultaneous presence of G-quadruplex-forming oligonucleotides and fragments of double-stranded genomic (calf thymus) DNA[14d] using competition experiments. We chose only one compound (**3**) from the disubstituted piperidinyl derivatives, while **5** and the two piperazinyl substituted molecules (**12** and **13**) were selected because they are the strongest quadruplex binders in this series. In particular, we wanted to obtain more information on these last two compounds as a consequence of the poor selectivity with DK66 as a duplex model. The results of these experiments are reported in Table 2. The choice of calculating the percentage of bound DNA has been made because this parameter is relevant to the specific biological activity of these compounds because, when referred to G-quadruplex DNA, it can be considered a measure of their capability to stabilize telomeric DNA in a G-quadruplex structure. This can prevent recognition and binding by telomerase, ultimately inhibiting telomerase activity.

Table 2. Competition Experiments on 21-TT Oligo[a]

	21-TT/CT				
compd	CT = 0	1:1	*N*%	1:5	*N*%
3	23 ± 3	19 ± 3	0.83	14 ± 5	0.61
5	56 ± 7	47 ± 3	0.84	39 ± 1	0.70
12	45 ± 3	40 ± 1	0.89	22 ± 1	0.49
13	48 ± 5	46 ± 1	0.96	32 ± 1	0.67
15	22 ± 3	13 ± 1	0.59	9 ± 1	0.41

[a] Values of percentage of bound 21-TT and normalized percentage of bound quadruplex (N%), as previously defined,[14d] for samples containing a fixed amount of both drug and G-quadruplex DNA (5 μM, 1:1 ratio) and different amounts of calf thymus DNA (CT), at the indicated quadruplex/duplex ratios (in phosphate ions) with standard deviations reported over at least three independent experiments.

All the studied compounds have high quadruplex selectivity, significantly better than **15**. In particular, **3**, although having the same affinity of **15** for 21-TT, has greater selectivity because at 1:1 duplex/quadruplex ratio the normalized percentage of bound quadruplex (*N*%) increased from 0.59 to 0.83 and at a 5:1 ratio from 0.41 to 0.61. The most impressive results are for **12** and **13**: both these compounds have *N*% values close to 1 at a 1:1 duplex/quadruplex ratio, in particular, **13**, despite their poor selectivity with duplex DK66. These results indicate that data obtained with a short duplex oligonucleotide may be misleading and are possibly physiologically irrelevant. This is not surprising, and we have already reported similar behavior for other compounds.[14d] We demonstrated that while those ligands showing a high level of selectivity between quadruplex and duplex oligonucleotides, confirming their selectivity in the competition experiment, the contrary was not always true: some ligands showing poor selectivity with the self-complementary dodecamer yet were selective in the presence of genomic DNA fragments. Undesired interactions between ligands and a short duplex DNA can include those with the terminal base pairs or with wider than usual grooves in proximity to the oligonucleotide ends or with a specific sequence of bases. On the contrary, genomic DNA is an uninterrupted long duplex structure and its sequence is not limited to a few base pairs but can be considered random over a large number of bases. The significant selectivity of **5** was confirmed, and because it also shows the highest percentage of bound DNA, it is the optimal compound of this series.

Thermal Stabilization of Quadruplex and Duplex DNA Using FRET Assays. The new perylene derivatives were also studied by fluorescence resonance energy transfer (FRET) assays because this technique is useful for evaluating their capability to stabilize quadruplex and duplex DNA structure against thermal denaturation.[16] Two fluorescent probes forming a donor−acceptor system have been linked to the ends of two oligonucleotides: the 21-mer human telomeric sequence F21T, as a G-quadruplex model, and a duplex forming a self-complementary decamer (T-loop, see Experimental Section for details). In this way, it is possible to rapidly obtain the difference between the melting temperature of DNA alone and in the presence of the compounds (ΔT_m), which is a measure of the thermal stabilization of the preformed DNA structures by them. ΔT_m values for the compounds studied at 1 μM concentration are reported in Table 3. At this concentration, all the molecules are able to stabilize the G-quadruplex structure, but to a different extent, while there are only negligible changes produced in the melting temperature of duplex DNA. These data are in good agreement with the binding study by ESI-MS. In particular, three

Table 3. Values of the Difference between the Melting Temperature of DNA Alone and in the Presence of the Drugs at 1 μM Concentration (ΔT_m)

	ΔT_m (°C)	
compd	F21T	T-loop
3	9.3 ± 0.5	−0.2 ± 0.3
4	13.1 ± 0.8	0.1 ± 0.2
5	23.0 ± 0.6	−0.2 ± 0.3
8	5.2 ± 0.1	−0.1 ± 0.2
9	16.6 ± 0.7	0.9 ± 0.4
10	12.9 ± 0.4	−0.4 ± 0.3
12	27.4 ± 0.3	2.9 ± 0.3
13	35.5 ± 0.6	2.3 ± 0.2
15	18.7 ± 0.8	0.2 ± 0.2

compounds show a higher ΔT_m than **15**: **5**, **12**, and **13**. They are the same compounds found to be the best quadruplex binders by ESI-MS experiments. The weakest binder of this series **8** shows the lowest ΔT_m value. It is concluded that even ithough the two methods investigate different features of drug−DNA interactions, there is a good correlation in this series of compounds between binding affinity for the G-quadruplex and thermal stabilization.

Effects on Telomere-Related Processes. The ability of the most promising perylene derivatives (**5**, **12**, and **13**) to inhibit human telomerase activity in comparison with **15**, was investigated in a cell-free system by means of a telomerase repeat amplification protocol (TRAP) assay (Figure 2). The TRAP assay used here is two-step: in the first, telomerase is allowed to elongate an oligonucleotide substrate, and in the second, PCR is used to amplify the elongation products. Because most quadruplex ligands can interfere with the PCR amplification of a sequence able to form a G-quadruplex, the TRAP assay has been performed by removing the inhibitor after telomerase extension. Figure 2A shows that, except for **15**, all the ligands are telomerase inhibitors but are effective at different concentrations. The IC_{50} values ranged from ca. 10−15 μM for **12** and **5**, while **13** was the most potent inhibitor with an IC_{50} of ca. 3 μM (Figure 2B). It is difficult to compare the IC_{50} values of our perylene derivatives with those of other G-quadruplex ligands available in the literature because, as already noted by various authors, the IC_{50} derived from this type of assay depends on the assay conditions and primer concentration.[17a,b,18] More importantly, many studies have used the TRAP assay without removing the inhibitor prior to the PCR step. As a consequence, the inhibitory effect of many quadruplex ligands has been overestimated. The limitations of the classic TRAP assay for the determination of telomerase inhibition by quadruplex ligands have been clearly demonstrated.[17b,18] For instance, telomestatin, one of the most potent G-quadruplex ligands, has an IC_{50} of 0.7 nM in classical TRAP conditions, whereas inhibition of telomerase obtained using the direct assay (without requiring the PCR step) occurs at a 1500-fold higher concentration.[18] These observations reinforce the notion that quadruplex ligands are more that simple telomerase inhibitors. Consistent with this hypothesis, G-quadruplex ligands have been found to show activity in telomerase-negative (ALT) tumor cell lines.[19]

Consequently, the ability of these ligands to directly uncap telomeres has been investigated. Human transformed fibroblasts (BJ-EHLT) were exposed to different concentrations of perylene derivatives for 24 h, and activation of damage response was

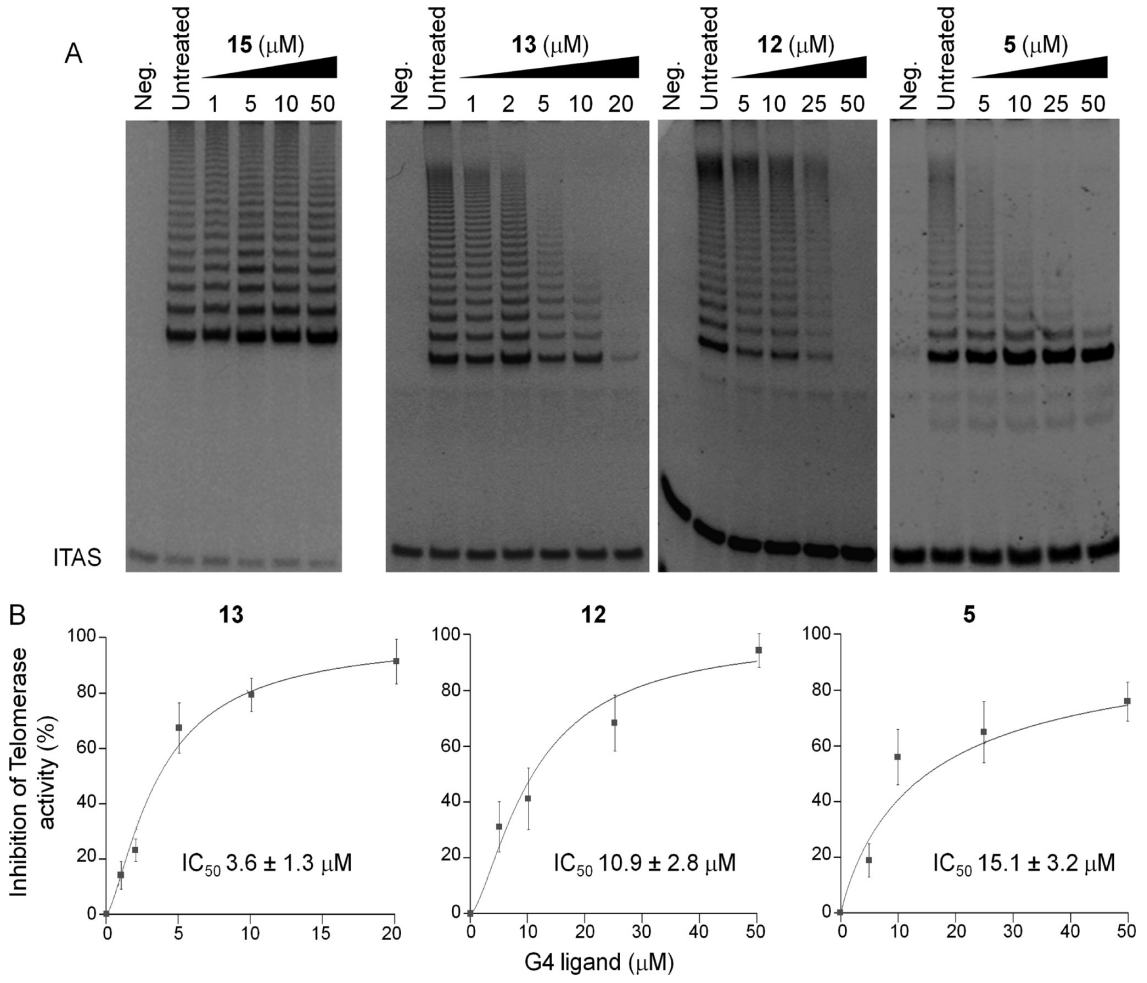

Figure 2. Inhibition of telomerase by perylene derivatives. Telomerase activity was evaluated by the telomerase repeat amplification protocol (TRAP) assay as reported in the Experimental Section. The compounds **15**, **12**, **13**, and **5** were added at different concentrations ranging from 1 to 50 μM. Before PCR, the samples were purified by phenol/chloroform extraction. Products were resolved on 12% PAGE and visualized with SYBR Green staining. (A) Representative TRAP assay. (B) Quantitative analysis was undertaken as reported in the Experimental Section and represents the mean of three independent experiments. The intensities of TRAP products were normalized to the intensities of the corresponding bands in the untreated sample. The percentage of telomerase inhibition was plotted against the concentrations used for each compound. IC_{50} values are reported inside each graph.

measured by immunofluorescence (Figure 3). We found that all the ligands induced strong phosphorylation of γ-H2AX, a hallmark of DNA double-strand break response (Figure 3A). Moreover, 53PB1, another DNA-damage response factor, was also activated upon exposure (Figure 3A), confirming that these compounds are DNA damage inducers. Strikingly, while for **15** activation of damage response in transformed cells occurred at a high concentration (3 μM), for **12**, **5**, and **13**, a dose of 0.25 μM was sufficient to induce γ-H2AX phosphorylation (Figure 3A). Moreover, while activation of γ-H2AX by **5** showed a well-defined signal, the γ-H2AX staining induced by **12** and **13** was diffuse, suggesting that these two ligands can induce nonspecific DNA damage (Figure 3B). Consistent with these observations, γ-H2AX and 53BPI were not significantly activated ($P > 0.05$) in normal telomerized fibroblasts (BJ-hTERT) upon treatment with **5**, even at the highest ligand concentration (Figure 3A). On the contrary, a dose-dependent increase ($P < 0.05$) in the percentage of γ-H2AX and 53BP1-positive cells was found in samples treated with either **12**, **13**, or **15** (Figure 3A).

On the basis of these results, we used BJ-EHLT cells treated with **5** (the most promising compound) to verify whether γ-H2AX was phosphorylated in response to dysfunctional telomeres. Deconvolution microscopy revealed that some of the damaged foci (both γ-H2AX and 53BP1) induced by **5** colocalized with TRF1, an effective marker for interphase telomeres,[20] forming so-called telomere-dysfunction induced foci (TIFs[21]) (Figure 3C). Quantitative analysis revealed that treatment with **5** significantly increased the percentage of cells ($p \leq 0.01$) with more than four γ-H2AX/TRF1 colocalizations (the percentage of TIFs-positive cells reached about 50% upon treatment with 1 μM concentration), with a mean of ca. five TIFs per nucleus (Figure 3D,E). Notably, an important fraction of the damage response is not colocalized at telomeres. Analysis of human genome composition has identified many G-quadruplex-forming sequences outside telomeres.[22] Therefore, it is possible then that **5** can also interact with additional G-quadruplex targets.

Notably, phosphorylation of γ-H2AX was restricted to a fraction of **5**-treated cells (ca. 50% at 0.5 μM concentration; see Figure 3A), suggesting that compound **5** can induce replication-dependent induction of DNA damage. To verify this hypothesis and determine which fraction of the cells formed γ = H2AX foci, we performed coimmunostaining to γ-H2AX and the proliferating cell nuclear antigen PCNA, which accumulates in the nucleus during S-phase.

dx.doi.org/10.1021/jm1013665 |J. Med. Chem. 2011, 54, 1140–1156

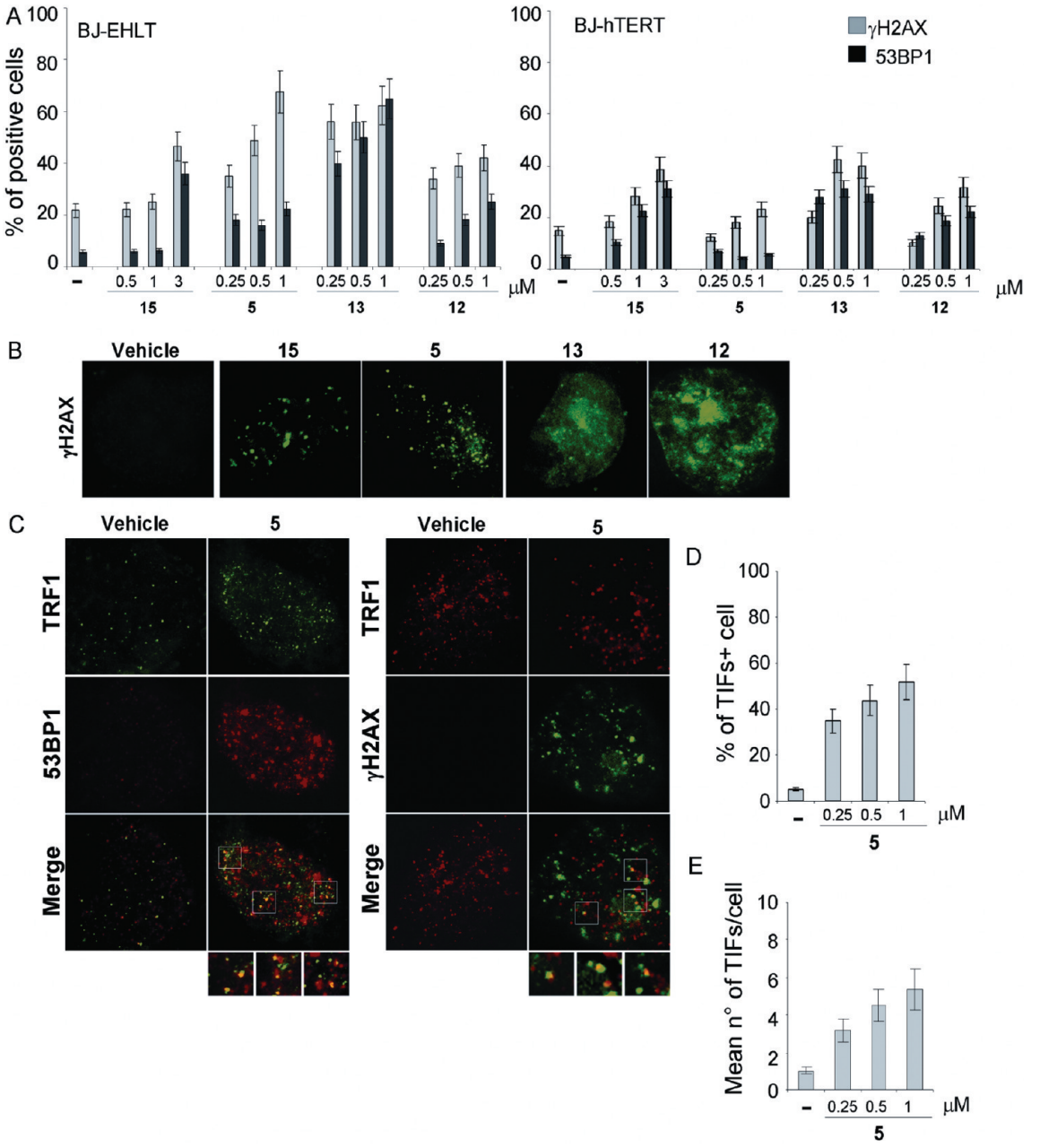

Figure 3. Activation of DNA damage response at telomeres by perylene derivatives. Transformed (BJ-EHLT) and normal telomerized (BJ-hTERT) human fibroblasts were treated with different concentrations of **15**, **12**, **13**, and **5** for 24 h, fixed, and processed for IF by using antibodies against γ-H2AX and 53PB1. (A) Quantitative analysis showing the percentage of γ-H2AX- and 53PB1-positive cells. Three independent experiments were evaluated, and error bars indicate the standard deviation. (B) Representative images of IF against γ-H2AX were acquired with a Leica Deconvolution microscope (magnification 100×). Untreated and **5**-treated BJ-EHLT cells were stained with TRF1 and γ-H2AX or 53BP1 and processed for IF. (C) Representative images of IF were acquired with a Leica Deconvolution microscope (magnification 100×). Enlarged views are reported below the merged images from **5**-treated groups. Percentage of TIFs-positive cells (D) and average number of TIFs per nucleus (E) in untreated and **5**-treated cells. Cells with four or more γ-H2AX/TRF1 foci were scored as TIF positive. The mean of three independent experiments is reported. Error bars indicate SD.

The results demonstrated that γ-H2AX foci formation was restricted to cells in S-phase; ca. 80% of cells positive for γ-H2AX being also positive for PCNA (Figure 4A,B). Moreover, to determine the cause of telomere uncapping, we investigated the effect of **5** on the localization of TRF1, TRF2, and POT1, three telomeric proteins that induce telomere dysfunction and evoke DNA damage signaling when their levels are reduced at telomeres. ChIP assay showed that **5** rapidly (24 h) delocalized POT1 from telomeres, and this effect was maintained after 72 h of treatment (Figure 4C,D). On the contrary, TRF1 and TRF2 remained associated with the telomeres upon treatment with ligand **5** (Figure 4C,D).

The ability of G-quadruplex ligands to uncap telomeres has been already described for other agents[7c,23], reinforcing the notion that these agents can act as broad inhibitors of telomere-related process and therefore the rationale for the development of this class of inhibitors as anticancer agents must be found elsewhere other than solely in the inhibition of telomerase expression. The shelter in complex may also be involved in the response of cells to this class of

dx.doi.org/10.1021/jm1013665 |J. Med. Chem. 2011, 54, 1140–1156

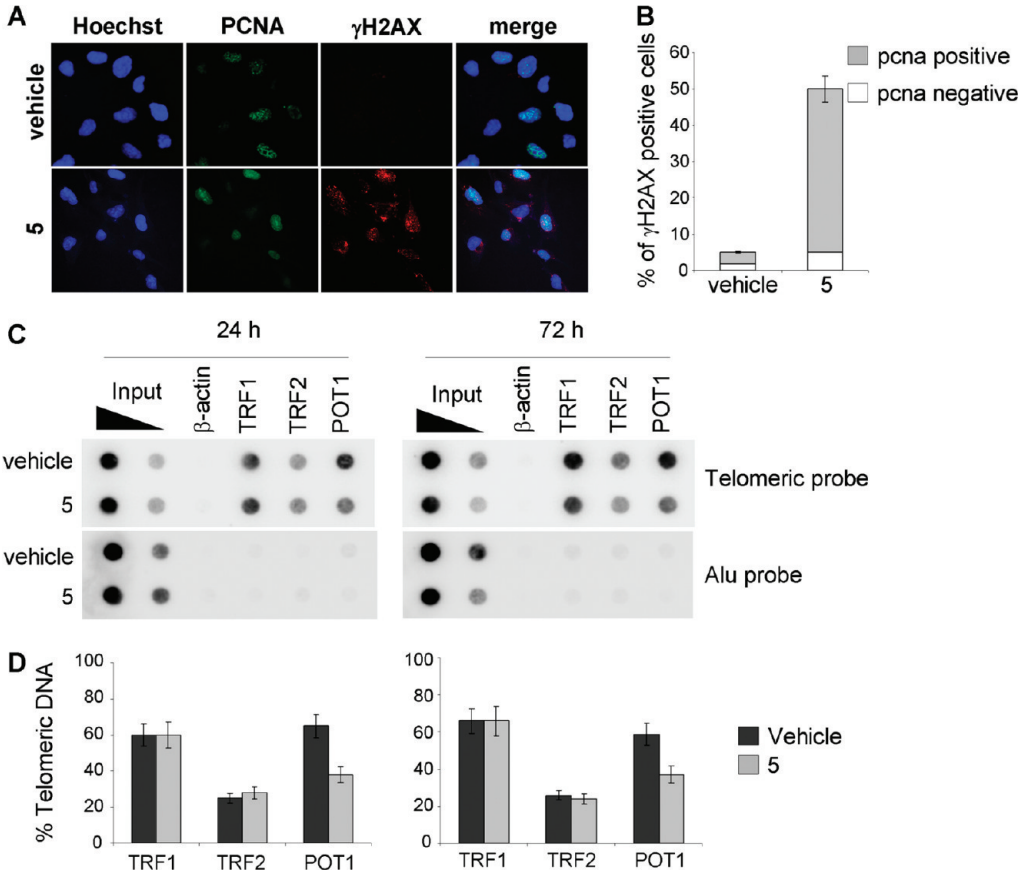

Figure 4. Replication-dependent damage induced by **5** is associated with POT1 dissociation from telomeres. BJ-EHLT fibroblasts treated with compound **5** and processed for IF and ChIP. (A) Representative images of IF against γ-H2AX and PCNA, acquired with a Leica Deconvolution microscope (magnification 63×), are reported. Hoechst staining was used to mark nuclei. (B) Percentage of γ-H2AX+/PCNA− or γ-H2AX+/PCNA+ nuclei in the indicated samples. The mean of three independent experiments with comparable results is shown. (C) Protein extracts from the indicated samples were subjected to ChIP analysis using antibodies against TRF1, TRF2, and POT1. β-actin antibody was used as negative control. The total DNA (input) represents 10% and 1% of genomic DNA. Southern blot analysis was performed by using telomeric or ALU repeat-specific probes. (D) The signals obtained were quantified by densitometry, and the percentage of precipitated DNA was calculated as a ratio of input signals and plotted. Four independent experiments were evaluated and error bars indicate the standard deviation.

agent. Indeed, we have previously reported that overexpression of either TRF2 or POT1 results in cells becoming resistant to the G-quadruplex ligand RHPS4 both in vitro and in nude mice.[7c] Therefore, analysis of the expression of these telomeric proteins may be predictive of the cellular response to G4-interactive compounds.

Effect on Cellular Proliferation and Tumor Survival. An important question concerns the selectivity of these ligands toward cancer cells. To answer this, we analyzed the antiproliferative effect of perylene derivatives on transformed and normal telomerized fibroblasts. Cells were exposed to the different compounds at the dose causing significant DNA damage when cells were exposed for 24 h: 0.5 μM concentration, for **12**, **13**, and **5** and 3 μM for **15** (Figure 5). A time-dependent decrease of cell proliferation was observed in transformed BJ-EHLT cells treated with all the ligands, reaching ca. 50% of growth inhibition at day 8 (Figure 5A,B). Inhibition of proliferation has been also found in the normal telomerized BJ-hTERT cells exposed to **12**, **13**, and **15** (Figure 5A and B). Interestingly, **5** did not have antiproliferative effect in normal fibroblasts, which were unaffected by the treatment, suggesting that this agent would preferentially limit the growth of cancer cells (Figure 5A,B). The selectivity of **5** for transformed cells has been also observed by comparing normal prostate versus PC3 prostate carcinoma cells (Figure 5C,D). In agreement with these results, cell cycle analysis of untreated and treated BJ-hTERT cells showed that **12** and **13** induced potent perturbation of the cell cycle, blocking the cells in G_2/M phase (Figure 6). On the contrary, **5** did not induce alteration of cells in the different phases of the cell cycle and DNA content was similar in untreated and drug-treated cells (Figure 6).

The selectivity of G-quadruplex ligands for cancer cells remains an intriguing issue in the telomere field. It may be that telomeres and their associated proteins (notably TRF2 and/or POT1) differ in protein expression levels between normal and cancer cells, and therefore the latter could be more or less accessible to these agents. Alternatively, the cellular response to these molecules could be different. Moreover, the selective effect of G-quadruplex ligands on transformed and cancer cells could result from a checkpoint failure that would allow the accumulation of deleterious DNA damage. The very early appearance of telomere damage and the subsequent detrimental effects on cell viability suggest that cells have to be chronically exposed to the drug to accumulate enough lethal damage. Whatever the precise reason, this differential response is intriguing and may open new avenues of investigation.

All the experiments performed on the different perylene derivatives identify compound **5** as the most promising selective

dx.doi.org/10.1021/jm1013665 |J. Med. Chem. 2011, 54, 1140–1156

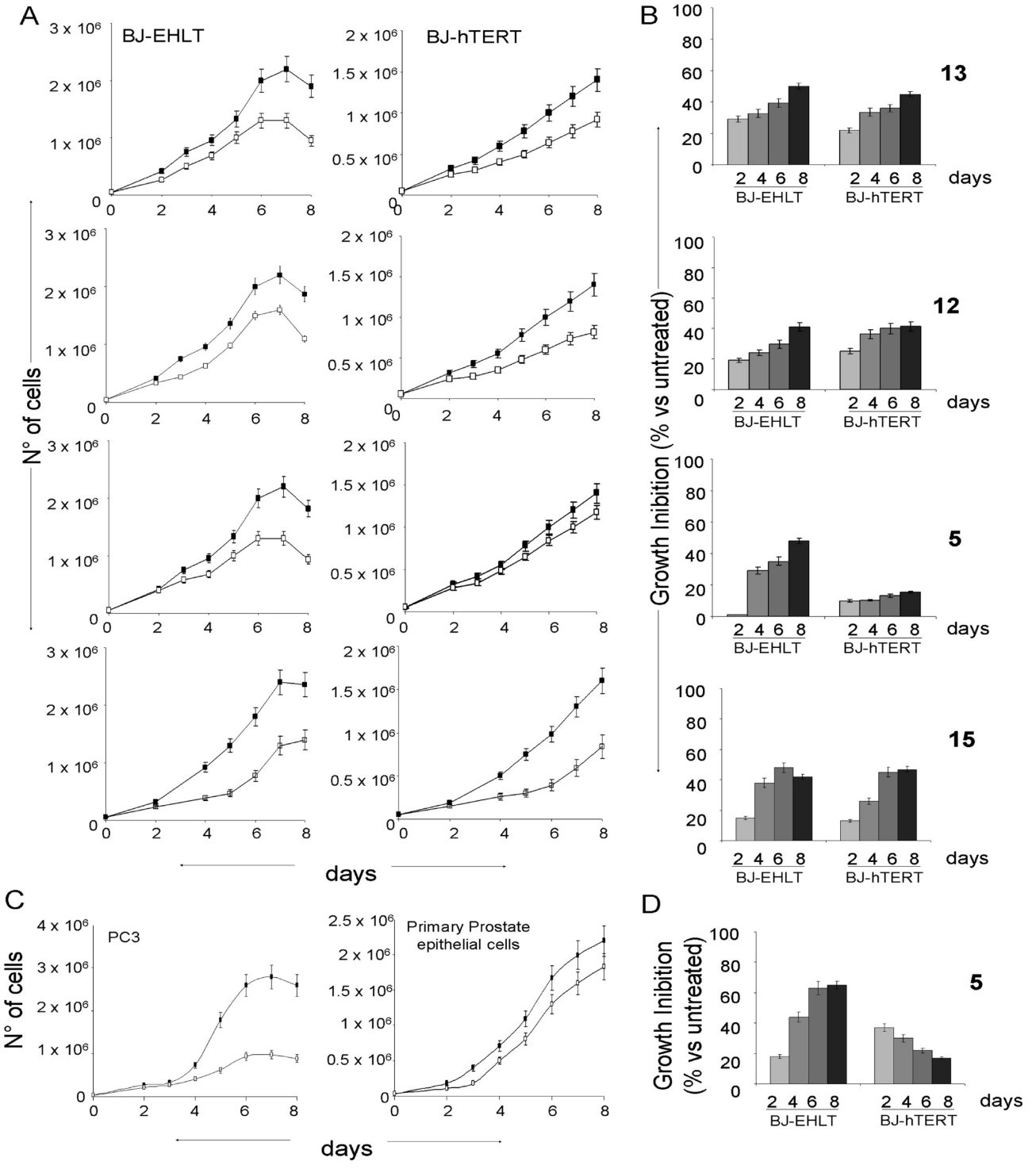

Figure 5. Antiproliferative effect of perylene derivatives on normal and transformed cells. Transformed (BJ-EHLT) and normal telomerized (BJ-hTERT) human fibroblasts were treated with **15**, **12**, **13**, and **5** perylene derivatives. (A) In vitro growth curves of the indicated lines untreated (■) and treated (□) with 0.5 μM (for **12**, **13**, and **5**) or 3 μM for **15**. (B) Percentage of growth inhibition of drug-treated vs untreated cells calculated at day 2, 4, 6, and 8 of culture. In vitro growth curves (C) and percentage of growth inhibition (D) of normal prostate epithelial cells and PC3 prostate carcinoma cell line treated with 0.5 μM of **5**. The figure shows representative experiments performed in quintuplicate with standard deviations (SD).

G4-interactive agent in this series, warranting further studies. We therefore decided to test the effect of **5** on tumor cell survival. The clonogenic assay is the most valid test to measure in vitro the fraction of cells that can survive after drug treatment and can be capable of repopulating a tumor after subcurative therapy. The analysis, performed on two cancer cell lines of different histotype, HT29 coloncarcinoma and M14 melanoma, revealed that compound **5** was able to inhibit cell survival in a dose-dependent manner (Figure 7). The IC_{50} values were similar in the two cancer lines, being ca. 1.1 and 0.8 μM for HT29 and M14 cells.

dx.doi.org/10.1021/jm1013665 |*J. Med. Chem.* 2011, 54, 1140–1156

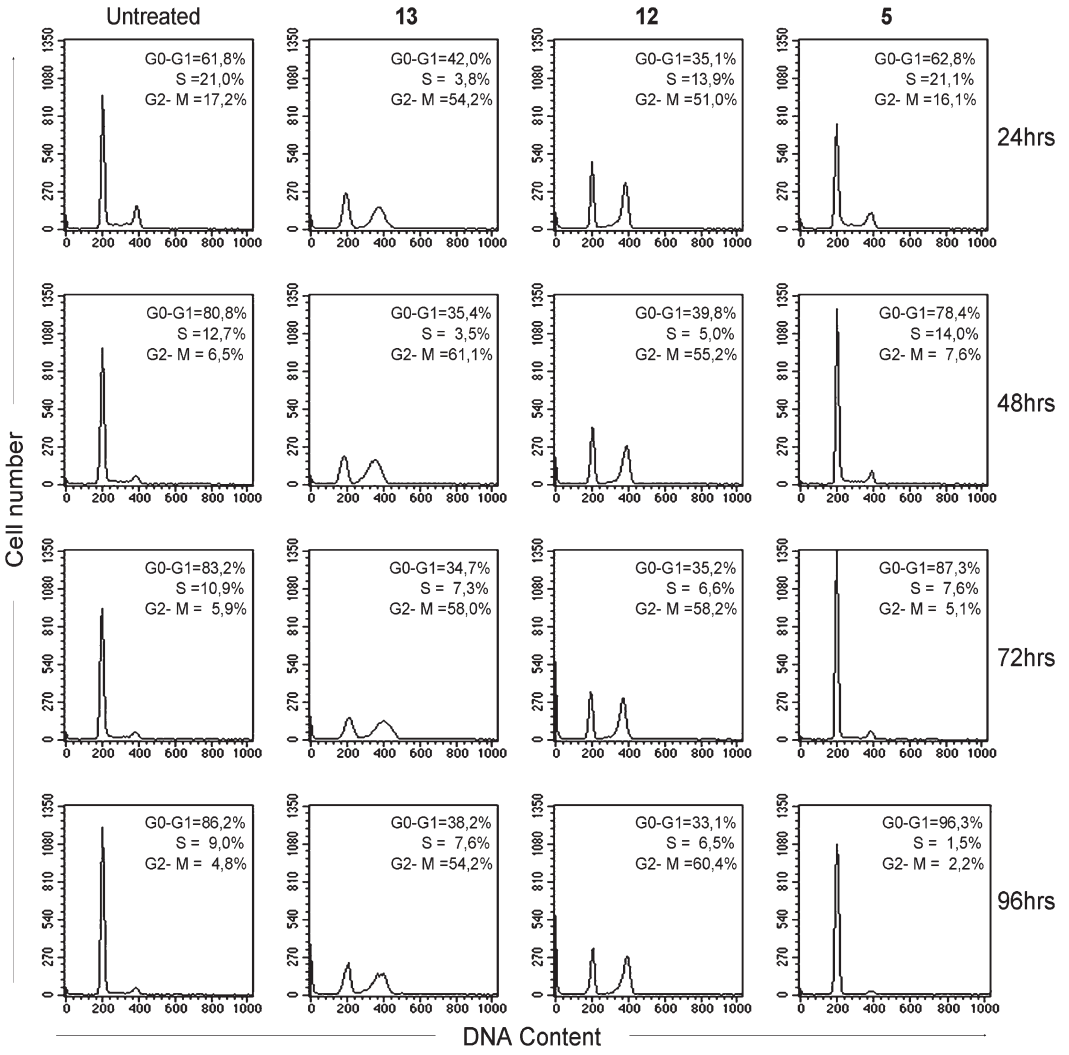

Figure 6. Effect of perylene derivatives on cell cycle of normal telomerized fibroblasts. Cell cycle analysis after PI staining was performed by flow cytometry at 24−96 h of treatment with 0.5 μM of the indicated perylene derivatives. The percentages of cells in the different phases of cell cycle were reported inside the relative histogram. A representative out of three independent experiments is shown.

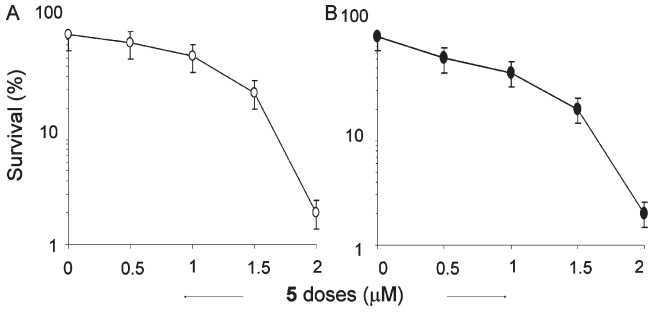

Figure 7. Effect of the G4 ligand **5** on tumor cell survival. Survival curves of HT29 coloncarcinoma (A) and M14 melanoma cell lines (B) exposed for 4 days to different doses of **5** ranging from 0.5 to 2 μM. Surviving fractions were calculated as the ratio of absolute survival of the treated sample/absolute survival of the control sample. The data represent the mean of four independent experiments with standard deviations (SD).

These interesting results need to be validated in in vivo experimental models of human cancers. In particular, the evaluation of toxicological profile and anticancer activity of this promising perylene derivative will permit us to assess its therapeutic index and to proceed along the development process to future clinical applications.

CONCLUSIONS

All the reported compounds are efficient G-quadruplex ligands as shown by ESI-MS measurements, with one major exception. They are also able to stabilize the human monomeric G-quadruplex structure formed in the presence of physiologically relevant K^+ ions, as found by FRET assay. In contrast to what we have previously found for simple perylene diimides with two side chains,[10,11] the modification of the ending groups or the length of the major axis side chains did not result in major changes in the affinity for the intramolecular quadruplex structure formed by the human telomeric sequence. On the contrary, the modification of the number or the nature of the groups directly bound to the bay area has a large influence on the activity of the perylene derivatives as G-quadruplex ligands. In particular, molecules with piperazinyl substituents or having only one piperidinyl group on the bay area showed significantly higher affinity for this G-quadruplex compared to the other compounds of this series. Even more interestingly, the last group of compounds also

dx.doi.org/10.1021/jm1013665 |J. Med. Chem. 2011, 54, 1140–1156

showed high selectivity for G-quadruplex with respect to duplex DNA in competition experiments with genomic DNA. Various biological assays have been performed on these compounds. The results demonstrated that compound **5** (the most interesting ligand with only one piperidinyl group in the bay area) triggered telomere damage in replicating cells, dissociated POT1 from telomeres, and appeared to preferentially kill transformed and cancer cells. Even though no mechanism has been described to fully explain the selectivity of these G-quadruplex ligands toward cancer cells, it appears to be a general phenomenon that characterizes this class of compounds. If future experiments will prove that only telomeres from cancer cells are affected and thus only cancer cells die, telomere-dependent strategies may provide a promising future anticancer treatment.

EXPERIMENTAL SECTION

1. Chemistry: General. All commercial reagents and solvents were purchased from Fluka and Sigma-Aldrich and used without further purification. TLC glass plates (silica gel 60 F_{254}) and silica gel 60 (0.040−0.063 mm) were purchased from Merck. ^{1}H and ^{13}C NMR spectra were performed with Varian Gemini 200 and Varian Mercury 300 instruments. ESI-MS spectra were recorded on a Micromass Q-TOF MICRO spectrometer. Elemental analyses (C, H, N) were carried out on EA1110 CHNS-O (CE instruments). Starting compounds **1** and **11**[13] were prepared as elsewhere described. All compounds used in the biophysical and biological evaluations were >95% pure as determined by HPLC (instrument, HPLC-Waters 2487; column, SUPELCO LC-Diol HPLC column, 5 μm particle size, L × I.D., 25 cm × 4.6 mm).

*1.2. Preparation of Compounds **3**−**5** (Scheme 1)*

1.2.1. N,N′-Bis(5-methanesulfonyl-3-oxapentyl)-1,7-dibromoperylene-3,4,9,10-tetracarboxylic Diimide (2). **1** (mixture of the two 1,6 and 1,7 isomers, 1.46 g) was dissolved in anhydrous dichloromethane (60 mL) and triethylamine (1.6 mL). Methanesulfonyl chloride (0.6 mL) was added dropwise at room temperature. The reaction mixture was then refluxed stirring under argon for 3 h. Successively, the organic layer was washed with water, HCl 0.5 M, saturated $NaHCO_3$ solution, and saturated NaCl solution. After treatment with anhydrous Na_2SO_4, the solvents were evaporated under vacuum to give 1.78 g (99% yield) of the product **2**.

^{1}H NMR (200 MHz, $CDCl_3$): δ 9.49 (d, J = 8 Hz, 2H, aromatic H), 8.91 (s, 2H, aromatic H), 8.70 (d, J = 8 Hz, 2H, aromatic H), 4.49 (broad, 4H, N-CH_2), 4.35 (broad, 4H, CH_2-O-S), 3.90 (broad, 4H, O-CH_2), 3.81 (broad, 4H, O-CH_2), 3.03 (s, 6H, S-CH_3) ppm. ^{13}C NMR ($CDCl_3$): δ 163.0 (C═O), 162.5 (C═O), 138.2 (aromatic), 133.1 (aromatic), 133.0 (aromatic), 130.2 (aromatic), 129.3 (aromatic), 128.7 (aromatic), 127.1 (aromatic), 123.2 (aromatic), 122.7 (aromatic), 121.0 (aromatic), 69.3, 68.8, 68.3, 39.7, 37.8 ppm.

1.2.2. Synthesis of 3, 4, and 5. One gram of compound **2**, actually a mixture of the two possible isomers, was stirred in piperidine (25 mL) at 95 °C under argon for 4 h. After cooling, water was added and the crude product was extracted with chloroform. The organic layer was extracted with water until the aqueous layer was neutral. After drying over Na_2SO_4 and evaporation in vacuum, the crude product was purified by column chromatography on silica gel ($CHCl_3$ saturated with aq NH_3) to give 500 mg (51% yield) of **3**, 180 mg (18% yield) of **4**, and 210 mg (24% yield) of **5**. The products were then crystallized by dissolving in a mixture of MeOH and 37% aqueous HCl solution 95:5 and precipitating the respective hydrochlorides with diethyl ether; 380 mg of hydrochloride were obtained starting from 430 mg of basic compound **3** (76% yield), 120 mg starting from 150 mg of basic compound **4** (68% yield), and 150 mg starting from 180 mg of basic compound **5** (70% yield).*N,N′*-Bis(5-(1-piperidino)-3-oxapentyl)-1,7-bis(1-piperidinyl)-perylene-3,4,9,10-tetracarboxylic Diimide Hydrochloride (**3**, PPL17). ^{1}H NMR (200 MHz, $CDCl_3$): δ 9.35 (d, J = 8 Hz, 2H, aromatic H), 8.26 (d, J = 8 Hz, 2H, aromatic H), 8.17 (s, 2H, aromatic H), 4.48 (broad, 4H, N_{imidic}-CH_2), 3.79 (broad, 4H, O-CH_2), 3.64 (broad, 4H, O-CH_2), 3.35 (m, 4H, C_{ar}-$N_{piperidine}$-CH_2), 2.75 (m, 4H, C_{ar}-$N_{piperidine}$-CH_2), 2.51 (broad, 4H, $N_{piperidine}$-CH_2), 2.35 (broad, 8H, $N_{piperidine}$-$CH_{2piperidine}$), 1.7−1.3 (broad, 24H, $CH_{2piperidine}$) ppm. ^{13}C NMR ($CDCl_3$): δ 163.7 (C═O), 163.7 (C═O), 151.0 (aromatic), 135.3 (aromatic), 129.6 (aromatic), 128.2 (aromatic), 124.1 (aromatic), 123.7 (aromatic), 123.3 (aromatic), 122.7 (aromatic), 122.4 (aromatic), 120.9 (aromatic), 69.0, 68.1, 58.8, 54.9, 52.9, 39.8, 26.1, 25.9, 24.5, 24.0 ppm. MS (ESI) m/z: 867.4789 [$(M + H)^+$] (calcd for $C_{52}H_{63}N_6O_6$ M = 867.4809). Anal. found C 61.8%, H 7.2%, N 8.2% (Calcd for [$C_{52}H_{62}N_6O_6 \cdot 2HCl \cdot 4H_2O$]: C 61.7%, H 7.2%, N 8.3%).*N,N′*-Bis(5-(1-piperidino)-3-oxapentyl)-1,6-bis(1-piperidinyl)-perylene-3,4,9,10-tetracarboxylic Diimide Hydrochloride (**4**, PPL16). ^{1}H NMR (200 MHz, $CDCl_3$): δ 9.70 (d, J = 8 Hz, 2H, aromatic H), 8.60 (d, J = 8 Hz, 2H, aromatic H), 8.36 (s, 2H, aromatic H), 4.48 (broad, 4H, N_{imidic}-CH_2), 3.82 (broad, 4H, O-CH_2), 3.67 (broad, 4H, O-CH_2), 3.35 (m, 4H, C_{ar}-$N_{piperidine}$-CH_2), 2.87 (m, 4H, C_{ar}-$N_{piperidine}$-CH_2), 2.52 (broad, 4H, $N_{piperidine}$-CH_2), 2.37 (broad, 8H, $N_{piperidine}$-$CH_{2piperidine}$), 1.8−1.3 (broad, 24H, $CH_{2piperidine}$) ppm. ^{13}C NMR ($CDCl_3$): δ 164.0 (C═O), 163.9 (C═O), 153.5 (aromatic), 136.3 (aromatic), 132.0 (aromatic), 131.0 (aromatic), 129.1 (aromatic), 128.2 (aromatic), 124.0 (aromatic), 123.4 (aromatic), 122.7 (aromatic), 121.0 (aromatic), 120.4 (aromatic), 69.0, 68.1, 68.0, 58.8, 55.1, 53.4, 39.6, 39.3, 26.1, 24.5, 24.0 ppm. MS (ESI) m/z: 867.4828 [$(M + H)^+$] (calcd for $C_{52}H_{63}N_6O_6$ M = 867.4809). Anal. found C 62.7%, H 7.1%, N 8.3% (Calcd for [$C_{52}H_{62}N_6O_6 \cdot 2HCl \cdot 3H_2O$]: C 62.8%, H 7.1%, N 8.5%).*N,N′*-Bis(5-(1-piperidino)-3-oxapentyl)-1,6-bis(1-piperidinyl)-perylene-3,4,9,10-tetracarboxylic Diimide Hydrochloride (**5**, PPL3C). ^{1}H NMR (200 MHz, $CDCl_3$): δ 9.80 (d, J = 8 Hz, 1H, aromatic H), 3.2 (m, 2H, aromatic H), 8.51 (m, 3H, aromatic H), 4.48 (broad, 4H, N_{imidic}-CH_2), 3.83 (broad, 4H, O-CH_2), 3.67 (broad, 4H, O-CH_2), 3.45 (m, 2H, C_{ar}-$N_{piperidine}$-CH_2), 2.91 (m, 2H, C_{ar}-$N_{piperidine}$-CH_2), 2.52 (broad, 4H, $N_{piperidine}$-CH_2), 2.37 (broad, 8H, $N_{piperidine}$-$CH_{2piperidine}$), 1.8−1.3 (broad, 18H, $CH_{2piperidine}$) ppm. ^{13}C NMR ($CDCl_3$): δ 163.4 (C═O), 163.2 (C═O), 152.4 (aromatic), 135.6 (aromatic), 134.4 (aromatic), 133.5 (aromatic), 131.0 (aromatic), 130.5 (aromatic), 128.8 (aromatic), 128.6 (aromatic), 128.2 (aromatic), 126.6 (aromatic), 125.0 (aromatic), 124.6 (aromatic), 124.3 (aromatic), 123.4 (aromatic), 123.2 (aromatic), 122.5 (aromatic), 122.1 (aromatic), 122.0 (aromatic), 121.3 (aromatic), 121.0 (aromatic), 68.7, 67.7, 58.5, 54.9, 52.9, 39.4, 39.3, 25.8, 25.7, 24.2, 23.6 ppm. MS (ESI) m/z: 784.4036 [$(M + H)^+$] (calcd for $C_{47}H_{54}N_5O_6$ M = 784.4074). Anal. found C 60.7%, H 7.1%, N 7.5% (Calcd for [$C_{47}H_{53}N_5O_6 \cdot 2HCl \cdot 4H_2O$]: C 60.8%, H 6.8%, N 7.5%).

*1.3. Preparation of Compounds **8**−**10** (Scheme 2)*

1.3.1. N,N′-Bis(5-hydroxy-3-oxapentyl)-1,7-bis(1-piperidinyl)perylene-3,4,9,10-tetracarboxylic Diimide (6). One gram of **1**, actually a mixture of the two possible isomers, was stirred in piperidine (15 mL) at 80 °C under argon for 4 h. After cooling, water was added and the crude product was extracted with chloroform. The organic layer was extracted with water until the aqueous layer was neutral. After drying over Na_2SO_4 and evaporation in vacuo, the crude product was purified by column chromatography on silica gel ($CHCl_3$:$(CH_3)_2CO$:MeOH 88:10:2) to give 718 mg (71% yield) of **6**, together with 80 mg (18%) of the corresponding 1,6 isomer.*N,N′*-Bis(5-hydroxy-3-oxapentyl)-1,7-bis(1-piperidinyl)perylene-3,4,9,10-tetracarboxylic Diimide (**6**). ^{1}H NMR (200 MHz, $CDCl_3$): δ 9.34 (d, J = 8 Hz, 2H, aromatic H), 8.28 (d, J = 8 Hz, 2H, aromatic H), 8.18 (s, 2H, aromatic H), 4.48 (t, J = 5.5 Hz, 4H, N-CH_2), 3.90 (t, J = 5.5 Hz, 4H, O-CH_2), 3.70 (m, 8H, O-CH_2) 3.33 (m, 4H, $N_{piperidine}$-CH), 2.75 (m, 4H, $N_{piperidine}$-CH), 1,72 (broad, 8H, $N_{piperidine}$-CH_2-CH_2), 1.38 (broad, 4H, $N_{piperidine}$-CH_2-CH_2-CH_2) ppm. ^{13}C NMR ($CDCl_3$): δ 163.7 (C═O), 163.7 (C═O), 150.5 (aromatic), 135.0 (aromatic), 129.5 (aromatic), 127.8 (aromatic), 123.8 (aromatic), 123.5 (aromatic), 123.0 (aromatic), 122.3

(aromatic), 121.9 (aromatic), 120.4 (aromatic), 72.4, 68.6, 61.8, 52.6, 39.9, 25.7, 23.7 ppm. MS (ESI) *m/z*: 733.3205 [(M + H)$^+$] (calcd for $C_{42}H_{45}N_4O_8$ M = 733.3237).*N,N′*-Bis(5-hydroxy-3-oxapentyl)-1,6-bis-(1-piperidinyl)perylene-3,4,9,10-tetracarboxylic Diimide. ^{1}H NMR (200 MHz, $CDCl_3$): δ 9.71 (d, *J* = 8 Hz, 2H, aromatic H), 8.62 (d, *J* = 8 Hz, 2H, aromatic H), 8.62 (s, 2H, aromatic H), 4.49 (broad, 4H, N-CH_2), 3.90 (broad, 4H, O−CH_2), 3.73 (m, 8H, O−CH_2) 3.38 (m, 4H, $N_{piperidine}$-CH), 2.88 (m, 4H, $N_{piperidine}$-CH), 1,86 (broad, 8H, $N_{piperidine}$-CH_2-CH_2), 1.46 (broad, 4H, $N_{piperidine}$-CH_2-CH_2-CH_2) ppm. ^{13}C NMR ($CDCl_3$): δ 163.6 (C═O), 152.6 (C═O), 135.8 (aromatic), 131.0 (aromatic), 130.3 (aromatic), 129.0 (aromatic), 128.7 (aromatic), 128.2 (aromatic), 127.2 (aromatic), 123.7 (aromatic), 123.1 (aromatic), 122.4 (aromatic), 121.8 (aromatic), 119.3 (aromatic), 71.7, 67.9, 67.7, 61.2, 52.5, 39.1, 38.8, 25.1, 23.1 ppm.

1.3.2. N,N′-Bis(5-methanesulfonyl-3-oxapentyl)-1,7-bis(1-piperidinyl)-perylene-3,4,9,10-tetracarboxylic Diimide (7). First, 500 mg of **6** were dissolved in anhydrous dichloromethane (20 mL) and triethylamine (195 μL). Methanesulfonyl chloride (130 μL) was added dropwise at 0 °C. The reaction mixture was then stirred for 2 h at room temperature. Successively, the organic layer was washed with water, HCl 0.5 M, saturated $NaHCO_3$ solution, and saturated NaCl solution. After treatment with anhydrous Na_2SO_4, the solvents were evaporated under vacuum to give 586 mg (95% yield) of the product **7**.

^{1}H NMR (200 MHz, $CDCl_3$): δ 9.50 (d, *J* = 8 Hz, 2H, aromatic H), 8.34 (d, *J* = 8 Hz, 2H, aromatic H), 8.30 (s, 2H, aromatic H), 4.48 (broad, 4H, N-CH_2), 4.35 (broad, 4H, CH_2-O-S), 3.85 (m, 8H, O-CH_2), 3.43 (m, 4H, $N_{piperidine}$-CH), 3.02 (s, 6H, S-CH_3), 2.88 (m, 4H, $N_{piperidine}$-CH), 1.79 (broad, 8H, $N_{piperidine}$-CH_2-CH_2), 1.45 (broad, 4H, $N_{piperidine}$-CH_2-CH_2-CH_2) ppm.

1.3.3. Synthesis of 8, 9, and 10—general Procedure. A mixture of compound **7** and the suitable amine, together with the specified solvents when appropriate, was stirred in the reported conditions. After cooling, dichloromethane was added and the organic layer was extracted with water until the aqueous layer was neutral. The crude product was purified by column chromatography on silica gel ($CHCl_3$:MeOH:aqueous NH_3 solution 98:2:0.2) and then crystallized by dissolving in a mixture of MeOH and 37% aqueous HCl solution 95:5 and precipitating the respective hydrochloride with diethyl ether.1.3.3.1. *N,N′*-Bis(5-(4-methyl-1-piperazino)-3-oxapentyl)-1,7-bis(1-piperidinyl)-perylene-3,4,9,10-tetracarboxylic Diimide Hydrochloride (**8**, PPLMPPZ). First, 100 mg of compound **7** were reacted with 4 mL of 1-methylpiperazine for 1 h at 60 °C under argon. The reaction workup as described above gave 88 mg (87% yield) of **8**, from which the respective hydrochloride (30 mg, 29% yield) was obtained.

^{1}H NMR (300 MHz, $CDCl_3$): δ 9.53 (d, *J* = 8 Hz, 2H, aromatic H), 8.35 (m, 4H, aromatic H), 4.45 (t, *J* = 5 Hz, 4H, N_{imidic}-CH_2), 3.78 (m, 8H, O-CH_2), 3.44 (broad, 4H, $N_{piperidine}$-CH), 2.96 (m, 20H, $N_{piperazine}$-CH_2), 2.76 (broad, 4H, $N_{piperidine}$-CH_2), 2.59 (s, 6H, $N_{piperazine}$-CH_3) 1,78 (broad, 8H, $N_{piperidine}$-CH_2-CH_2), 1.44 (broad, 4H, $N_{piperidine}$-CH_2-CH_2-CH_2) ppm. ^{13}C NMR ($CDCl_3$): δ 163.6 (C═O), 163.5 (C═O), 150.7 (aromatic), 135.4 (aromatic), 129.77 (aromatic), 127.9 (aromatic), 124.0 (aromatic), 123.6 (aromatic), 123.1 (aromatic), 122.7 (aromatic), 122.1 (aromatic), 120.6 (aromatic), 68.1, 67.9, 57.1, 53.7, 52.7, 51.4, 44.5, 39.2, 25.7, 23.7 ppm. MS (ESI) *m/z*: 897.5016 [(M + H)$^+$] (calcd for $C_{52}H_{65}N_8O_6$ M = 897.5027). Anal. found C 50.6%, H 6.5%, N 9.8% (Calcd for [$C_{52}H_{64}N_8O_6$·6HCl·6H_2O]: C 51.0%, H 6.8%, N 9.2%).1.3.3.2. *N,N′*-Bis(5-dimethylamino-3-oxapentyl)-1,7-bis(1-piperidinyl)-perylene-3,4,9,10-tetracarboxylic Diimide Hydrochloride (**9**, PPLDMA). Compound **7** (100 mg) was dissolved in anhydrous dioxane (5 mL), and then a 33% THF solution of dimethylamine (5 mL) was added. The reaction mixture was then stirred for 18 h at 70 °C under argon. The reaction workup as described above gave 44 mg (45% yield) of **9**, from which the respective hydrochloride (44 mg, 82% yield) was obtained.

^{1}H NMR (300 MHz, $CDCl_3$): δ 9.44 (d, *J* = 8 Hz, 2H, aromatic H), 8.32 (2, 2H, *J* = 8 Hz, aromatic H), 8.26 (s, 2H, aromatic H), 4.46 (t, *J* = 5.1 Hz, 4H, N_{imidic}-CH_2), 3.92 (t, *J* = 5.1 Hz, 4H, O−CH_2), 3.85 (t, *J* = 5.1 Hz, 4H, O-CH_2), 3.41 (broad, 4H, $N_{piperidine}$-CH), 3.05 (t, *J* = 5.1 Hz, 4H, N_{aminic}-CH_2), 2.83 (broad, 4H, $N_{piperidine}$-CH_2), 2.67 (s, 12H, N-CH_3) 1,75 (broad, 8H, $N_{piperidine}$-CH_2-CH_2), 1.43 (broad, 4H, $N_{piperidine}$-CH_2-CH_2-CH_2) ppm. ^{13}C NMR ($CDCl_3$): δ 163.4 (C═O), 163.3 (C═O), 150.6 (aromatic), 135.0 (aromatic), 129.5 (aromatic), 127.7 (aromatic), 123.8 (aromatic), 123.4 (aromatic), 123.0 (aromatic), 122.4 (aromatic), 122.0 (aromatic), 120.6 (aromatic), 68.1, 68.0, 58.4, 52.7, 45.3, 39.4, 25.7, 23.7 ppm. MS (ESI) *m/z*: 787.4178 [(M + H)$^+$] (calcd for $C_{46}H_{55}N_6O_6$ M = 787.4183). Anal. found C 58.1%, H 6.8%, N 8.8% (Calcd for [$C_{46}H_{54}N_6O_6$·2HCl·5H_2O]: C 58.1%, H 7.0%, N 8.8%).1.3.3.3. *N,N′*-Bis(5-methylamino-3-oxapentyl)-1,7-bis(1-piperidinyl)-perylene-3,4,9,10-tetracarboxylic Diimide Hydrochloride (**10**, PPLMA). Compound **7** (89 mg) was dissolved in dioxane (5 mL), and then a 33% aqueous solution of methylamine (5 mL) was added. The reaction mixture was then stirred for 90 min at 60 °C under argon. The reaction workup as described above gave 53 mg (73% yield) of **10**, from which the respective hydrochloride (35 mg, 55% yield) was obtained.

^{1}H NMR (300 MHz, $CDCl_3$): δ 9.31 (d, *J* = 8 Hz, 2H, aromatic H), 8.27 (2, 2H, *J* = 8 Hz, aromatic H), 8.17 (s, 2H, aromatic H), 4.46 (broad, 4H, N_{imidic}-CH_2), 3.88 (m, 8H, O-CH_2), 3.33 (broad, 4H, $N_{piperidine}$-CH), 3.03 (broad, 4H, N_{aminic}-CH_2), 2.89 (broad, 4H, $N_{piperidine}$-CH_2), 2.88 (s, 6H, N-CH_3) 1,72 (broad, 8H, $N_{piperidine}$-CH_2-CH_2), 1.38 (broad, 4H, $N_{piperidine}$-CH_2-CH_2-CH_2) ppm. ^{13}C NMR ($CDCl_3$): δ 163.7 (C═O), 163.5 (C═O), 150.6 (aromatic), 135.2 (aromatic), 129.6 (aromatic), 128.0 (aromatic), 124.0 (aromatic), 123.6 (aromatic), 123.0 (aromatic), 122.6 (aromatic), 122.0 (aromatic), 120.5 (aromatic), 68.6, 68.4, 52.7, 50.5, 39.6, 29.7, 25.7, 23.7 ppm. MS (ESI) *m/z*: 759.3861 [(M + H)$^+$] (calcd. for $C_{44}H_{51}N_6O_6$ M = 759.3870). Anal. found C 58.4%, H 6.7%, N 9.1% (Calcd for [$C_{44}H_{50}N_6O_6$·2HCl·4H_2O]: C 58.5%, H 6.7%, N 9.3%).

*1.4. Preparation of Compounds **12**−**14** (Scheme 3)*

1.4.1. N,N′-Bis[2-(1-piperidino)-ethyl]-1,7-[4-methyl-1-piperazinyl]-perylene-3,4,9,10-tetracarboxylic Diimide Hydrochloride (12, 4CPPZ17). 50 mg of **11**,[13] actually a mixture of the two possible isomers, was stirred in 1-methyl piperazine (2.5 mL) at 40 °C under argon for 10 days. Then, water was added and the crude product was extracted with chloroform. The organic layer was extracted with water until the aqueous layer was neutral. After drying over Na_2SO_4 and evaporation in vacuum, the crude product was purified by column chromatography on silica gel ($CHCl_3$:MeOH 9:1) to give 39 mg (74% yield) of **12**. The product was then crystallized by dissolving in a mixture of MeOH and 37% aqueous HCl solution 95:5 and precipitating the respective hydrochloride (33 mg) with diethyl ether (85% yield).

^{1}H NMR (200 MHz, $CDCl_3$): δ 9.44 (d, *J* = 8 Hz, 2H, aromatic H), 8.32 (d, *J* = 8 Hz, 2H, aromatic H), 8.21 (s, 2H, aromatic H), 4.44 (t, *J* = 6 Hz, 4H, N_{imidic}-CH_2), 3.37 (broad, 4H, C_{ar}-$N_{piperazine}$-CH_2), 2.96 (broad, 4H, C_{ar}-$N_{piperazine}$-CH_2), 2.78 (broad, 12H, $N_{piperidine}$-CH_2), 2.40 (broad, 14H, $N_{piperazine}$-CH), 1.72 (broad, 8H, $N_{piperidine}$ CH_2-CH_2), 1.52 (broad, 24H, $N_{piperidine}$-CH_2-CH_2-CH_2) ppm. ^{13}C NMR ($CDCl_3$): δ 163.2 (C═O), 163.2 (C═O), 149.6 (aromatic), 134.5 (aromatic), 129.5 (aromatic), 127.8 (aromatic), 123.9 (aromatic), 123.3 (aromatic), 122.8 (aromatic), 122.4 (aromatic), 122.2 (aromatic), 120.8 (aromatic), 56.1, 54.7, 54.6, 51.0, 46.0, 37.4, 30.0, 25.6, 24.1 ppm. MS (ESI) *m/z*: 809.4485 [(M + H)$^+$] (calcd for $C_{48}H_{57}N_8O_4$ M = 809.4503). Anal. found C 51.5%, H 6.8%, N 9.7% (Calcd for [$C_{48}H_{56}N_8O_4$·6HCl·5H_2O]: C 51.6%, H 6.5%, N 10.0%).

1.4.2. N,N′-Bis[2-(1-piperidino)-ethyl]-1-[4-(3-dimethylaminopropyl)-1-piperazinyl]-perylene-3,4,9,10-tetracarboxylic Diimide Hydrochloride (13, 3CPPZS). First, 100 mg of **11**,[13] actually a mixture of the two possible isomers, was stirred in 1-(3-dimethylaminopropyl)piperazine (650 mg) and anhydrous dioxane at 80 °C under argon for 7 h. After cooling, water was added and the crude product was extracted with chloroform. The organic layer was extracted with water until the aqueous

layer was neutral. After drying over Na_2SO_4 and evaporation in vacuo, the crude product was purified by column chromatography on silica gel ($CHCl_3$:MeOH:aqueous NH_3 solution 9:1:0.2) to give 33 mg (32% yield) of **13**. The product was then crystallized by dissolving in a mixture of MeOH and 37% aqueous HCl solution 95:5 and precipitating the respective hydrochloride (33 mg) with diethyl ether (85% yield).

^{1}H NMR (200 MHz, $CDCl_3$): δ 9.45 (d, J = 8 Hz, 1H, aromatic H), 8.5−8.2 (m, 6H, aromatic H), 4.38 (m, 4H, N_{imidic}-CH_2), 3.23 (broad, 2H, C_{ar}-$N_{piperazine}$-CH_2), 2.82 (m, 20H, C_{ar}-$N_{piperazine}$-CH_2, $N_{piperidine}$-CH_2, $N_{piperazine}$-$CH_{2piperazine}$), 2.57 (m, 8H, $N_{piperazine}$-CH_2, N-CH_3), 1.71 (broad, 8H N-CH_2-$CH_{2piperidine}$), 1.50 (broad, 8H, N-CH_2-CH_2-CH_2) ppm. ^{13}C NMR ($CDCl_3$): δ 163.2 (C═O), 163.0 (C═O), 162.9 (C═O), 151.2 (aromatic), 135.0 (aromatic), 134.0 (aromatic), 133.3 (aromatic), 130.9 (aromatic), 130.3 (aromatic), 128.5 (aromatic), 128.3 (aromatic), 126.3 (aromatic), 124.6 (aromatic), 124.5 (aromatic), 124.2 (aromatic), 123.6 (aromatic), 123.1 (aromatic), 122.3 (aromatic), 122.0 (aromatic), 121.9 (aromatic), 121.5 (aromatic), 120.9 (aromatic), 56.8, 55.7, 54.5, 54.4, 52.7, 51.1, 44.1, 25.3, 25.2, 23.8, 23.2 ppm. MS (ESI) m/z: 782.4368 [$(M + H)^+$] (calcd for $C_{47}H_{56}N_7O_4$ M = 782.4394). Anal. found C 53.2%, H 6.7%, N 8.7% (Calcd for [$C_{47}H_{55}N_7O_4 \cdot 5HCl \cdot 5H_2O$]: C 53.5%, H 6.7%, N 9.3%).

1.4.3. N,N′-Bis[2-(1-piperidino)-ethyl]-1,7-[4-(3-dimethylamino-propyl)-1-piperazinyl]-perylene-3,4,9,10-tetracarboxylic Diimide (14, 4CPPZS). 50 mg of **11**,[13] actually a mixture of the two possible isomers, was stirred in 1-(3-dimethylaminopropyl)piperazine (5 mL) at room temperature under argon for 7 days. Then, water was added and the crude product was extracted with chloroform. The organic layer was extracted with water until the aqueous layer was neutral. After drying over Na_2SO_4 and evaporation in vacuum, the crude product was purified by column chromatography on silica gel ($CHCl_3$:MeOH 9:1) to give 17 mg (28% yield) of **14**, together with 10 mg (20% yield) of **13**.

^{1}H NMR (300 MHz, $CDCl_3$): δ 9.45 (d, J = 8 Hz, 2H, aromatic H), 8.30 (d, J = 8 Hz, 2H, aromatic H), 8.24 (s, 2H, aromatic H), 4.37 (t, J = 8.8 Hz, 4H, N_{imidic}-CH_2), 3.23 (broad, 2H, C_{ar}-$N_{piperazine}$-CH_2), 2.82 (m, 20H, C_{ar}-$N_{piperazine}$-CH_2, $N_{piperidine}$-CH_2, $N_{piperazine}$-$CH_{2piperazine}$), 2.57 (m, 8H, $N_{piperazine}$-CH_2, N-CH_3), 1.71 (broad, 8H N-CH_2-$CH_{2piperidine}$), 1.50 (broad, 8H, N-CH_2-CH_2-CH_2) ppm. ^{13}C NMR ($CDCl_3$): δ 163.5 (C═O), 163.5 (C═O), 149.9 (aromatic), 135.0 (aromatic), 129.9 (aromatic), 128.2 (aromatic), 124.4 (aromatic), 123.7 (aromatic), 123.2 (aromatic), 122.8 (aromatic), 122.7 (aromatic), 121.2 (aromatic), 57.8, 56.7, 56.6, 54.9, 53.2, 53.1, 51.4, 46.9, 45.4, 45.3, 37.9 ppm.

2. Determination of the Complexes between Ligands and Quadruplex/Duplex DNA by Electrospray Ionization Mass Spectrometry (ESI-MS). Single-stranded oligonucleotides were purchased from Eurofins MWG Operon (Ebersberg, Germany). Their sequences are: 5′-GGGTTAGGGTTAGGGTTAGGGTT-3′ (21-TT) and 5′-CGTAAATTTACG-3′ (DK66). ESI-MS spectra were recorded on a Micromass Q-TOF MICRO spectrometer (now Waters) in the negative ionization mode. The rate of sample infusion into the mass spectrometer was 5 μL/min, and the capillary voltage was set to −2.6 kV. The source temperature was adjusted to 70 °C, the cone voltage to 30 V, and the collision energy to 5 V. Data were analyzed using the MassLynx software developed by Waters. Samples were prepared by mixing appropriate volumes of 150 mM ammonium acetate buffer, 50 μM annealed oligonucleotide stock solution, 100 μM stock solutions of perylene or coronene derivatives, and methanol. The final concentration of DNA in each sample was 5 μM (in duplex or quadruplex unit), and the final volume of the sample was 50 μL. Drugs were added at different drug/DNA ratios, ranging between 0.5 and 4. Methanol was added to the mixture just before injection (as 15% w/vol) after the binding equilibrium in ammonium acetate was established, in order to obtain a stable electrospray signal. As a reference, samples containing only 5 μM DNA with no drug were prepared in each series. Samples for competition experiments were prepared following the procedure described above, adding an appropriate volume of CT solution. Final concentrations of quadruplex DNA and drug solutions were always 5 μM, and CT was added at two different duplex/quadruplex ratios (1 and 5), calculated on the basis of phosphate group concentrations. To minimize random errors, each experiment has been repeated at least three times under the same experimental conditions. Data were processed and averaged with the SIGMAPLOT software.

For drug−DNA complexes with 1:1 and 2:1 stoichiometry, which have been shown to be the main species present in solution in all the experiments, the formation of such complexes can be represented by two distinct equilibria, which are described by the following two equations: K_1 = [1:1]/([DNA] [drug]) and K_2 = [2:1]/([1:1] [drug]), where [DNA], [drug], [1:1], and [2:1] represent respectively the concentrations of the different species in solution:DNA (duplex or quadruplex depending on the oligonucleotide used), the ligand, and the 1:1 and 2:1 drug−DNA complexes at equilibrium. The association constants K_1 and K_2 can be calculated directly from the relative intensities of the corresponding peaks found in the mass spectra, with the assumption that the response factors of the oligonucleotides alone and of the drug−DNA complexes are the same, so that the relative intensities in the spectrum are supposed to be proportional to the relative concentrations in the injected solution.[14d] The percentage of bound DNA was calculated according to an equation developed by Brodbelt and coworkers,[14b] which represents the percentage of DNA bound ligand:

$$\%\text{bound DNA} = 100 \times ([1:1]+[2:1])/([\text{DNA}]+[1:1]+[2:1])$$

3. FRET Assays on Quadruplex and Duplex DNA. Fluorescent conjugated oligonucleotides were purchased from Oswel Ltd. (Southampton, UK). Their sequences are: 5′-FAM-d(GGG[TTAGGG]$_3$)-TAMRA-3′, for the telomeric G-quadruplex (F21T) and 5′-FAM-dTA-TAGCTATA-HEG-TATAGCTATA-TAMRA-3′(HEG linker: [(−CH_2-CH_2-O−)$_6$]), for the duplex model (T-loop). Oligonucleotides were initially diluted in 50 mM potassium cacodylate buffer (pH 7.4) to the 2× concentration (400 nM) and then annealed by heating to 85 °C for 5 min, followed by cooling to room temperature in the heating block. Ninety-six-well plates (MJ Research, Waltham, MA) were prepared by aliquoting 50 μL of the annealed DNA to each well, followed by 50 μL of the compound solutions. Measurements were made on a DNA Opticon Engine (MJ Research) with excitation at 450−495 nm and detection at 515−545 nm. Fluorescence readings were taken at intervals of 0.5 °C over the range 30−100 °C, with a constant temperature being maintained for 30 s prior to each reading to ensure a stable value. Final analysis of the data was carried out using a script written in the program Origin 7.0 (OriginLab Corp., Northampton, MA).

4. Cells and Culture Conditions. BJ fibroblasts expressing hTERT (BJ-hTERT) or hTERT and SV40 early region (BJ-HELT), M14 melanoma, and HT29 coloncarcinoma were obtained and maintained as previously reported.[7c] Primary postate epithelial cells and PC3 prostate carcinoma were purchased from ATCC and maintained as reported in the manufacture's instructions.

5. TRAP Assay. Telomerase enzyme activity was measured with the PCR-based TRAP kit (Chemicon International, MA, USA), as previously reported.[24] To define the sensitivity of the method and the semiquantitative relationship between protein concentration and ladder band intensity, different amounts of protein extract (from 0.01 to 2 μg) were used. Before the PCR step, to purify the elongated products and remove the bound ligands, extraction with phenol/chloroform/isoamyl-alcohol (50:49:1) was performed and DNA was precipitated overnight at −20 °C. Reaction products were amplified in the presence of a 36 bp ITAS, and each set of TRAP assay included a control reaction without extract (negative control). Samples were separated on 12% PAGE and visualized with SYBR Green staining (Sigma Aldrich, Milan, Italy).

Gels were acquired using a gel scanner and intensity data were obtained by ImageQuant software. Quantitative analysis was performed by integrating the total intensity of each PCR product ladder. The values obtained were corrected for background by subtracting the signal intensity of negative controls. Data for all ligands were collected at a range of concentrations to obtain dose−response curves from which the IC_{50} values (the concentration required for 50% enzyme inhibition) were calculated by Calcusyn software.

6. Immunofluorescence. Immunofluorescence was performed as previously reported.[7c] Cells were fixed in 2% formaldehyde and permeabilized in 0.25% Triton X100 in PBS for 5 min at room temperature. For immunolabeling, cells were incubated with primary antibody and then washed in PBS and incubated with the fluorophore-conjugated secondary antibodies. The following primary antibodies were used: pAb and mAb anti-TRF1 (Abcam Ltd.; Cambridge UK), mAb anti-γ-H2AX (Upstate, Lake Placid, NY), pAb anti-53BP1 (Novus Biologicals Inc., Littleton, CO), and mAb anti-PCNA (Sigma). The following secondary antibodies were used: Texas Red conjugated goat anti-rabbit, fluorescein conjugated goat anti-mouse (Jackson Laboratory). Fluorescence signals were captured by using a Leica DMIRE2 microscope equipped with a Leica DFC 350FX camera and analyzed by Leica FW4000 deconvolution software (Leica, Solms, Germany).

7. Chromatin Immunoprecipitation (ChIP). ChIP assay was performed as previously described.[7c] Briefly, formaldehyde cross-linked chromatin fragments were immunoprecipitated with pAb anti-TR1 (Santa Cruz Biotechnology, Santa Cruz, CA), mAb anti-TRF2 (Imgenex, San Diego, CA), and pAb anti POT1 (Abcam). mAb anti-β-actin (Sigma) was used as a negative control for the ChIP assay. After precipitation with each antibody, the precipitants were blotted onto Hybond-N membrane (Amersham International, Buckinghamshire, UK) and telomeric repeat sequences were detected with TeloTAGGG probe. A nonspecific probe (ALU) was also used. The filter was exposed to a phosphoimager screen, and the signals were measured using ImageQuant software.

8. Proliferation Assays. Cells (5×10^4) were seeded in 60 mm Petri plates (Nunc, Mascia Brunelli, Milano, Italy), and 24 h after plating, freshly dissolved perylene derivatives were added to the culture medium. Cell counts (Coulter Counter, Kontron Instruments, Milano, Italy) and viability (trypan blue dye exclusion) were determined daily from day 1 to day 8 of culture.

9. Flow Cytometric Analysis. Cell cycle analysis was performed by flow cytometry (Becton-Dickinson, Heidelberg, Germany). Adherent cells (2×10^5) were fixed and resuspended in a solution containing propidium iodide (PI) at the concentration of 50 μg/mL. Cell percentages in the different phases of the cell cycle were measured using CELLQuest software (Becton Dickinson).

10. Clonogenic Assay. Cells were seeded in 60 mm Petri dishes (Nunc, Mascia Brunelli, Milan, Italy) at a density of 2×10^5 cells per dish and exposed to **5** for 4 days. Cell colony-forming ability was determined as previously described.[24] All the experiments were repeated four times in triplicate.

11. Statistical Analysis. The experiments have been repeated from three to five times, and the results obtained are presented as means ± SD. Significant changes were assessed by using Student's *t* test for unpaired data, and *P* values <0.05 were considered significant.

AUTHOR INFORMATION

Corresponding Author

*For M.F.: phone, +39-0649913341; fax, +39-064462778; E-mail, marco.franceschin@uniroma1.it. For A.B.: phone, +39-06-52662569; fax, +39-06-52662592; E-mail, biroccio@ifo.it.

ACKNOWLEDGMENT

This work was supported by MIUR (PRIN), Sapienza Università di Roma, Italian Association for Cancer Research (AIRC), and Ministero della Salute. E.S. and M.P. are recipients of fellowships from Italian Foundation for Cancer Research (FIRC). S.N. is supported by Cancer Research UK. Thanks are due to Prof. Maria Savino for constant helpful discussion.

ABBREVIATIONS USED

ESI-MS, electrospray ionization mass spectrometry; FRET, fluorescence resonance energy transfer; TRAP, telomerase repeat amplification protocol; TIFs, telomere-dysfunction induced foci; TRF1 or TRF2, telomeric repeat binding factor 1 or 2; POT1, protection of Telomeres 1; hTERT, human telomerase reverse transcriptase; 53BP1, p53 binding protein 1; PCNA, proliferating cell nuclear antigen; CT, calf thymus DNA

REFERENCES

(1) (a) Burge, S.; Parkinson, G. N.; Hazel, P.; Todd, A. K.; Neidle, S. Quadruplex DNA: sequence, topology and structure. *Nucleic Acids Res.* **2006**, *34*, 5402–5415. (b) Neidle, S.; Parkinson, G. N. Quadruplex DNA crystal structures and drug design. *Biochimie* **2008**, *90*, 1184–1196.

(2) Paeschke, K.; Simonsson, T.; Postberg, J.; Rhodes, D.; Lipps, H. J. Telomere end-binding proteins control the formation of G-quadruplex DNA structures in vivo. *Nature Struct. Mol. Biol.* **2005**, *12*, 847–854.

(3) Granotier, C.; Pennarun, G.; Riou, L.; Hoffschir, F.; Gauthier, L. R.; De Cian, A.; Gomez, D.; Mandine, E.; Riou, J. F.; Mergny, J. L.; Mailliet, P.; Dutrillaux, B.; Boussin, F. D. Preferential binding of a G-quadruplex ligand to human chromosome ends. *Nucleic Acids Res.* **2005**, *33*, 4182–4190.

(4) Neidle, S.; Parkinson, G. N. Telomere maintenance as a target for anticancer drug discovery. *Nature Rev. Drug Discovery* **2002**, *1*, 383–393.

(5) Franceschin, M. G-quadruplex DNA structures and organic chemistry: more than one connection. *Eur. J. Org. Chem.* **2009**, 2225–2238.

(6) (a) Riou, J. F.; Guittat, L.; Mailliet, P.; Laoui, A.; Renou, E.; Petitgenet, O.; Mégnin-Chanet, F.; Hélène, C.; Mergny, J. L. Cell senescence and telomere shortening induced by a new series of specific G-quadruplex DNA ligands. *Proc. Natl. Acad. Sci. U.S.A.* **2002**, *99*, 2672–2677. (b) Leonetti, C.; Amodei, S.; D'Angelo, C.; Rizzo, A.; Benassi, B.; Antonelli, A.; Elli, R.; Stevens, M. F.; D'Incalci, M.; Zupi, G.; Biroccio, A. Biological activity of the G-quadruplex ligand RHPS4 (3,11-difluoro-6,8,13-trimethyl-8*H*-quino[4,3,2-*kl*]acridinium methosulfate) is associated with telomere capping alteration. *Mol. Pharmacol.* **2004**, *66*, 1138–1146.

(7) (a) Neidle, S.; Read, M. A. G-quadruplexes as therapeutic targets. *Biopolymers* **2000−2001**, *56*, 195–208. (b) Riou, J. F. G-quadruplex interacting agents targeting the telomeric G-overhang are more than simple telomerase inhibitors. *Curr. Med. Chem. Anticancer Agents* **2004**, *4*, 439–443. (c) Salvati, E.; Leonetti, C.; Rizzo, A.; Scarsella, M.; Mottolese, M.; Galati, R.; Sperduti, I.; Stevens, M. F.; D'Incalci, M.; Blasco, M.; Chiorino, G.; Bauwens, S.; Horard, B.; Gilson, E.; Stoppacciaro, A.; Zupi, G.; Biroccio, A. Telomere damage induced by the G-quadruplex ligand RHPS4 has an antitumor effect. *J. Clin. Invest.* **2007**, *117*, 3236–3247.

(8) (a) Drygin, D.; Siddiqui-Jain, A.; O'Brien, S.; Schwaebe, M.; Lin, A.; Bliesath, J.; Ho, C. B.; Proffitt, C.; Trent, K.; Whitten, J. P.; Lim, J. K.; Von Hoff, D.; Anderes, K.; Rice, W. G. Anticancer activity of CX-3543: a direct inhibitor of rRNA biogenesis. *Cancer Res.* **2009**, *69*, 7653–61. (b) Bates, P. J.; Laber, D. A.; Miller, D. M.; Thomas, S. D; Trent, J. O. Discovery and development of the G-rich oligonucleotide AS1411 as a novel treatment for cancer. *Exp. Mol. Pathol.* **2009**, *86*, 151–164.

(9) (a) Micheli, E.; D'Ambrosio, D.; Franceschin, M.; Savino, M. Water soluble cationic perylene derivatives as possible telomerase inhibitors: the search for selective G-quadruplex targeting. *Mini-Rev. Med. Chem.* **2009**, *9*, 1622–1632. (b) Fedoroff, O. Y.; Salazar, M.; Han, H.; Chemeris, V. V.; Kerwin, S. M.; Hurley, L. H. NMR-based model of a telomerase-inhibiting compound bound to G-quadruplex DNA. *Biochemistry* **1998**, *37*, 12367–12374. (c) Kern, J. T.; Thomas, P. W.;

Kerwin, S. M. The relationship between ligand aggregation and G-quadruplex DNA selectivity in a series of 3,4,9,10-perylenetetracarboxylic acid diimides. *Biochemistry* **2002**, *41*, 11379–11389. (d) Tuntiwechapikul, W.; Taka, T.; Bétencourt, M.; Makonkawkeyoon, L.; Randall, L. T. The influence of pH on the G-quadruplex binding selectivity of perylene derivatives. *Bioorg. Med. Chem. Lett.* **2006**, *16*, 4120–4126.

(10) (a) Rossetti, L.; Franceschin, M.; Bianco, A.; Ortaggi, G.; Savino, M. Perylene diimides with different side chains are selective in inducing different G-quadruplex DNA structures and in inhibiting telomerase. *Bioorg. Med. Chem. Lett.* **2002**, *12*, 2527–2533. (b) Rossetti, L.; Franceschin, M.; Schirripa, S.; Bianco, A.; Ortaggi, G.; Savino, M. Selective interactions of perylene derivatives having different side chains with inter- and intramolecular G-quadruplex structures. A correlation with telomerase inhibition. *Bioorg. Med. Chem. Lett.* **2005**, *15*, 413–420.

(11) (a) Franceschin, M.; Lombardo, C. M.; Pascucci, E.; D'Ambrosio, D.; Micheli, E.; Bianco, A.; Ortaggi, G.; Savino, M. The number and distances of positive charges of polyamine side chains in a series of perylene diimides significantly influence their ability to induce G-quadruplex structures and inhibit human telomerase. *Bioorg. Med. Chem.* **2008**, *16*, 2292–2304. (b) Micheli, E.; Lombardo, C. M.; D'Ambrosio, D.; Franceschin, M.; Neidle, S.; Savino, M. Selective G-quadruplex ligands: the significant role of side chain charge density in a series of perylene derivatives. *Bioorg. Med. Chem. Lett.* **2009**, *19*, 3903–3908.

(12) (a) Alvino, A.; Franceschin, M.; Cefaro, C.; Borioni, S.; Ortaggi, G.; Bianco, A. Synthesis and spectroscopic properties of highly water-soluble perylene derivatives. *Tetrahedron* **2007**, *63*, 7858–7865. (b) Franceschin, M.; Pascucci, E.; Alvino, A.; D'Ambrosio, D.; Bianco, A.; Ortaggi, G.; Savino, M. New highly hydrosoluble and not self-aggregated perylene derivatives with three and four polar side chains as G-quadruplex telomere targeting agents and telomerase inhibitors. *Bioorg. Med. Chem. Lett.* **2007**, *17*, 2515–2522.

(13) Franceschin, M.; Alvino, A.; Ortaggi, G.; Bianco, A. New hydrosoluble perylene and coronene derivatives. *Tetrahedron Lett.* **2004**, *45*, 9015–9020.

(14) (a) Rosu, F.; De Pauw, E.; Gabelica, V. Electrospray mass spectrometry to study drug−nucleic acids interactions. *Biochimie* **2008**, *90*, 1074–1087. (b) Mazzitelli, C. L.; Brodbelt, J. S.; Kern, J. T.; Rodriguez, M.; Kerwin, S. M. Evaluation of binding of perylene diimide and benzannulated perylene diimide ligands to DNA by electrospray ionization mass spectrometry. *J. Am. Soc. Mass Spectrom.* **2006**, *17*, 593–604. (c) Rosu, F.; Gabelica, V.; Houssier, C.; Colson, P.; Pauw, E. D. Triplex and quadruplex DNA structures studied by electrospray mass spectrometry. *Rapid Commun. Mass Spectrom.* **2002**, *16*, 1729–1736. (d) Casagrande, V.; Alvino, A.; Bianco, A.; Ortaggi, G.; Franceschin, M. Study of binding affinity and selectivity of perylene and coronene derivatives towards duplex and quadruplex DNA by ESI-MS. *J. Mass Spectrom.* **2009**, *44*, 530–540.

(15) (a) Zhao, Y.; Wasielewski, M. R. 3,4:9,10-Perylenebis-(dicarboximide) chromophores that function as both electron donors and acceptors. *Tetrahedron Lett.* **1999**, *40*, 7047–7050. (b) Ahrens, M. J.; Tauber, M. J.; Wasielewski, M. R. Bis(*n*-octylamino)perylene-3,4:9,10-bis(dicarboximide)s and their radical cations: synthesis, electrochemistry, and ENDOR spectroscopy. *J. Org. Chem.* **2006**, *71*, 2107–2114.

(16) Mergny, J. L.; Maurizot, J. C. Fluorescence resonance energy transfer as a probe for G-quartet formation by a telomeric repeat. *Chembiochem* **2001**, *2*, 124–132.

(17) (a) Cathers, B. E.; Sun, D.; Hurley, L. H. Accurate determination of quadruplex binding affinity and potency of G-quadruplex-interactive telomerase inhibitors by use of a telomerase extension assay requires varying the primer concentration. *Anti-Cancer Drug Des.* **1999**, *14*, 367–372. (b) Reed, J. E.; Gunaratnam, M.; Beltran, M.; Reszka, A. P.; Vilar, R.; Neidle, S. TRAP-LIG, a modified TRAP assay to quantitate telomerase inhibition by small molecules. *Anal. Biochem.* **2008**, *380*, 99–105.

(18) De Cian, A.; Cristofari, G.; Reichenbach, P.; De Lemos, E.; Monchaud, D.; Teulade-Fichou, M. P.; Shin-Ya, K.; Lacroix, L.; Lingner, J.; Mergny, J. L. Reevaluation of telomerase inhibition by quadruplex ligands and their mechanism of action. *Proc. Natl. Acad. Sci. U.S.A.* **2007**, *14*, 17347–17352.

(19) (a) Gowan, S. M.; Heald, R.; Stevens, M. F.; Kelland, L. R. Potent inhibition of telomerase by small-molecule pentacyclic acridines capable of interacting with G-quadruplexes. *Mol. Pharmacol.* **2001**, *60*, 981–988. (b) Pennarun, G.; Granotier, C.; Gauthier, L. R.; Gomez, D.; Hoffschir, F.; Mandine, E.; Riou, J. F.; Mergny, J. L.; Mailliet, P.; Boussin, F. D. Apoptosis related to telomere instability and cell cycle alterations in human glioma cells treated by new highly selective G-quadruplex ligands. *Oncogene* **2005**, *24*, 2917–2928.

(20) van Steensel, B.; de Lange, T. Control of telomere length by the human telomeric protein TRF1. *Nature* **1997**, *385*, 740–743.

(21) Takai, H.; Smogorzewska, A.; de Lange, T. DNA damage foci at dysfunctional telomeres. *Curr. Biol.* **2003**, *13*, 1549–1556.

(22) (a) Todd, A. K.; Johnston, M.; Neidle, S. Highly prevalent putative quadruplex sequence motifs in human DNA. *Nucleic Acids Res.* **2005**, *33*, 2901–2907. (b) Huppert, J. L.; Balasubramanian, S. Prevalence of quadruplexes in the human genome. *Nucleic Acids Res.* **2005**, *33*, 2908–2916.

(23) (a) Burger, A. M.; Dai, F.; Schultes, C. M.; Reszka, A. P.; Moore, M. J.; Double, J. A.; Neidle, S. The G-quadruplex-interactive molecule BRACO-19 inhibits tumor growth, consistent with telomere targeting and interference with telomerase function. *Cancer Res.* **2005**, *65*, 1489–96. (b) Tauchi, T.; Shin-ya, K.; Sashida, G.; Sumi, M.; Okabe, S.; Ohyashiki, J. H.; Ohyashiki, K. Telomerase inhibition with a novel G-quadruplex interactive agent, telomestatin: in vitro and in vivo studies in acute leukemia. *Oncogene* **2006**, *25*, 5719–2.

(24) Biroccio, A.; Amodei, S.; Benassi, B.; Scarsella, M.; Cianciulli, A.; Mottolese, M.; Del Bufalo, D.; Leonetti, C.; Zupi, G. Reconstitution of hTERT restores tumorigenicity in melanoma-derived c-Myc low-expressing clones. *Oncogene* **2002**, *21*, 3011–3019.